

A Survey on Deep Learning Technique for Video Segmentation

Wenguan Wang, Tianfei Zhou, Fatih Porikli, *Fellow IEEE*, David Crandall, Luc Van Gool

Abstract—Video segmentation, *i.e.*, partitioning video frames into multiple segments or objects, plays a critical role in a broad range of practical applications, from enhancing visual effects in movie, to understanding scenes in autonomous driving, to virtual background creation in video conferencing, just to name a few. Recently, due to the renaissance of connectionism in computer vision, there has been an influx of deep learning based approaches for video segmentation that have delivered compelling performance. In this survey, we comprehensively review two basic lines of research — generic object segmentation (of unknown categories) in videos and video semantic segmentation — by introducing their respective task settings, background concepts, perceived need, development history, and main challenges. We also provide a detailed overview of representative literature on both methods and datasets. Additionally, we present quantitative performance comparisons of the reviewed methods on benchmark datasets. Finally, we point out a set of unsolved open issues in this field, and suggest possible opportunities for further research.

Index Terms—Video Segmentation, Video Object Segmentation, Video Semantic Segmentation, Deep Learning

1 INTRODUCTION

VIDEO segmentation — identifying the set of key objects (with some specific feature properties or semantic value) in a video scene — is a fundamental and challenging problem in machine vision. Due to its crucial role in widespread application areas (*e.g.*, autonomous driving, robotics, automated surveillance, social media, augmented reality, movie production, video conferencing, *etc.*), it has long garnered significant attention and been actively investigated in computer vision and graphics communities.

Video segmentation has been addressed in the past using various traditional computer vision and machine learning techniques, including hand-craft features (*e.g.*, color, histogram statistics, optical flow, *etc.*), heuristic prior knowledge (*e.g.*, visual attention mechanism [1], motion boundaries [2], *etc.*), low-/mid-level visual representations (*e.g.*, super-voxel [3], trajectory [4], object proposal [5], *etc.*), and classical machine learning models (*e.g.*, clustering algorithms [6], graph models [7], random walks [8], support vector machines [9], random decision forests [10], markov random fields [11], conditional random fields [12], *etc.*). Recently, deep neural networks, and Fully Convolutional Networks (FCNs) [13] in particular, have led to remarkable advances in video segmentation. These deep learning-based video segmentation algorithms have surpassed the more traditional approaches by a large margin in terms of accuracy and sometimes even efficiency, and continue to improve on the state-of-the-art.

With the rapid advance of this field, there is a huge body of new literature being produced. However, most existing surveys predate the modern deep learning era [14], [15], and often with a narrow view, *i.e.*, focusing on video

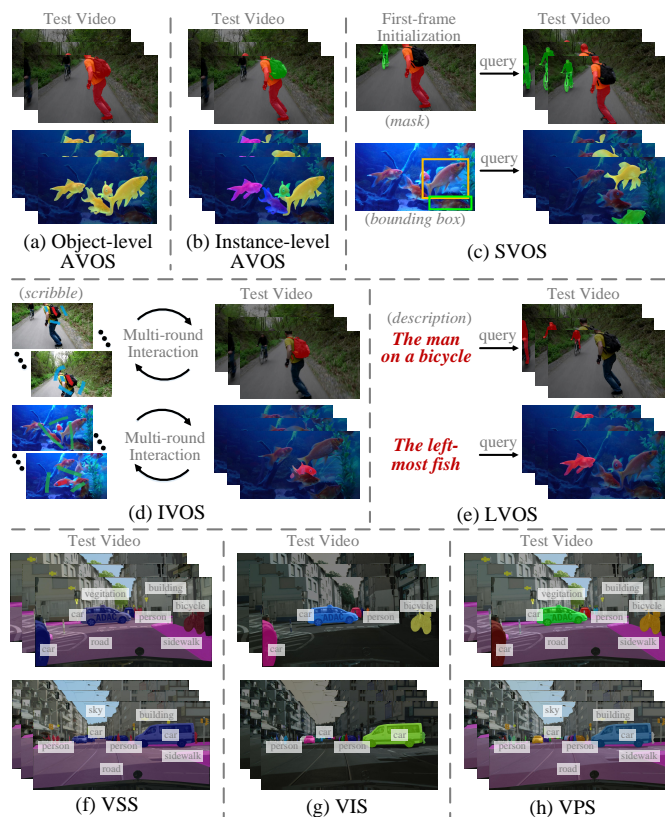


Fig. 1. Video segmentation tasks reviewed in this survey: (a) object-level automatic video object segmentation (object-level AVOS), (b) instance-level automatic video object segmentation (instance-level AVOS), (c) semi-automatic video object segmentation (SVOS), (d) interactive video object segmentation (IVOS), (e) language-guided video object segmentation (LVOS), (f) video semantic segmentation (VSS), (g) video instance segmentation (VIS), and (h) video panoptic segmentation (VPS).

foreground/background segmentation only [16], [17]. There is a need for a state-of-the-art review that addresses the wide area of video object segmentation, especially to help new researchers catch up on the rapidly-developing evolution

- W. Wang, T. Zhou, and L. Van Gool are with ETH Zurich. (Email: {wenguan.wang, ztfei.debug}@gmail.com, vangool@vision.ee.ethz.ch)
- F. Porikli is with the School of Computer Science, Australian National University. (email: fatih.porikli@anu.edu.au)
- D. Crandall is with the Luddy School of Informatics, Computing, and Engineering, the Indiana University. (email: djcran@indiana.edu)

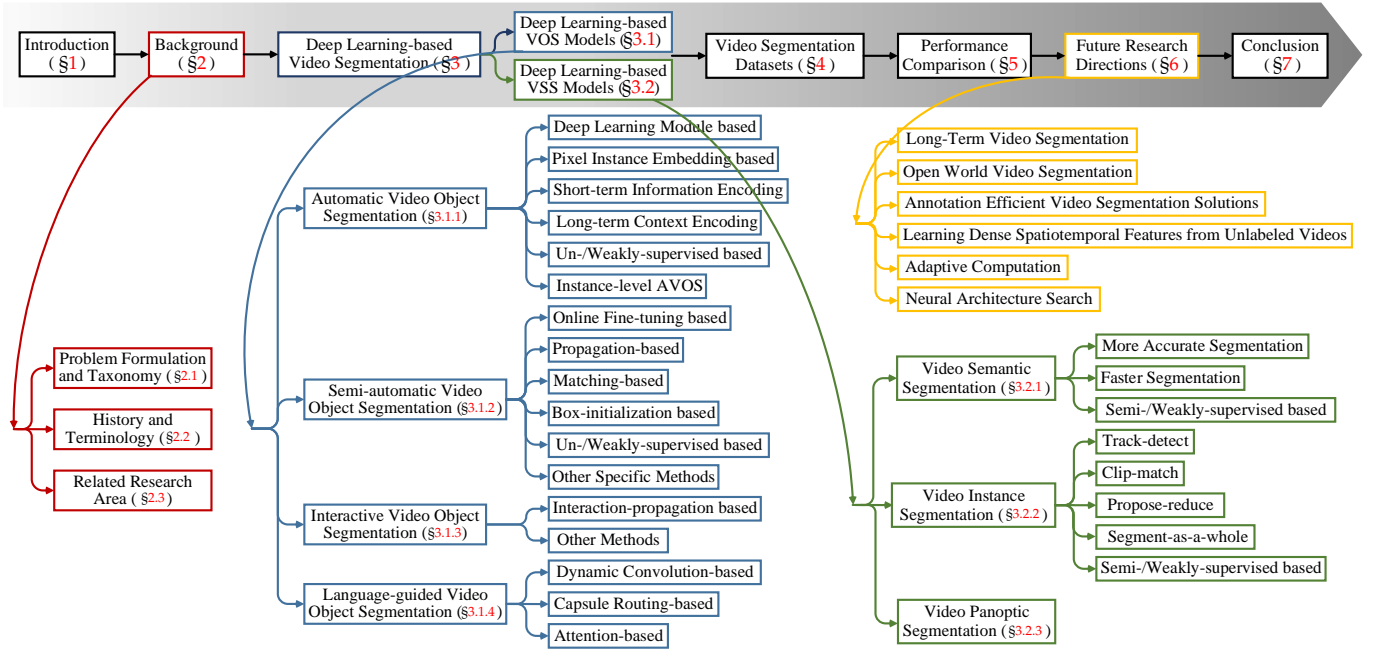


Fig. 2. Overview of this survey.

of the field. In response, we provide the first review that systematically introduces recent advance on video segmentation, spanning from task formulation to taxonomy, from algorithms to datasets, from unsolved issues to future research directions. It covers several crucial aspects, including task categories (*i.e.*, foreground/background separation *vs* semantic segmentation), inference modes (*i.e.*, automatic, semi-automatic, and interactive), and learning paradigms (*i.e.*, supervised, unsupervised, and weakly supervised), as well as clarifies confusing terminology (*e.g.*, background subtraction, motion segmentation, *etc.*). We hope that this survey will provide a comprehensive review for researchers, and foster research on the open issues raised.

This survey mainly focuses on recent progress in two major branches of video segmentation, namely video object segmentation (Fig. 1(a-e)) and video semantic segmentation (Fig. 1(f-h)), which can be further divided into eight sub-fields. Even after restricting our focus to deep learning-based video segmentation, there are still hundreds of papers in this rapidly growing field. We select influential papers published in prestigious journals and conferences. We also include some non-deep learning video segmentation models and relevant literature in other areas, *e.g.*, video object detection and visual tracking, to give necessary background.

Fig. 2 shows the structure of this survey. §2 gives some brief background on taxonomy, terminology, study history and related research areas. Representative papers on deep learning algorithms and video segmentation datasets are reviewed in §3 and §4, respectively. §5 conducts performance evaluation and analysis, while §6 raises open questions and directions. Finally, conclusion remarks are given in §7.

2 BACKGROUND

§2.1 formulates the task, categorizes research directions, and enumerates their key challenges and driving factors. §2.2 provides a brief historical background covering early work and foundations. §2.3 establishes linkages to the progress of other relevant fields.

2.1 Problem Formulation and Taxonomy

Formally, let \mathcal{X} and \mathcal{Y} denote the input space and output segmentation space, respectively. Deep learning-based video segmentation solutions generally seek to learn an *ideal* video-to-segment mapping $f^*: \mathcal{X} \mapsto \mathcal{Y}$.

2.1.1 Video Segmentation Category

According to the definitions of the output space \mathcal{Y} , video segmentation can be broadly categorized into two classes: video object (foreground/background) segmentation, and video semantic segmentation, which identify appropriate objects to satisfy the specific needs of different applications.

- **Video Foreground/Background Segmentation (Video Object Segmentation, VOS).** VOS, as the most classic video segmentation setting, refers to segmenting the dominant, general objects (of unknown categories) in video sequences. Thus \mathcal{Y} is a binary, foreground/background segmentation space. VOS is typically used in some video analysis and editing related application scenarios, such as object removal in movie editing, content-based video coding, and virtual background creation in video conferencing; it does not concern the exact semantic categories of the segmented objects.

- **Video Semantic Segmentation (VSS).** As a direct extension of image semantic segmentation to the spatio-temporal domain, VSS aims to extract objects within predefined semantic categories (*e.g.*, car, building, pedestrian, road) from videos. Thus, \mathcal{Y} corresponds to a multi-class, semantic parsing space. VSS serves as a perception foundation for many application fields, such as robot sensing, human-machine interaction, and autonomous driving, which require high-level understanding of the physical environment.

Remark. VOS and VSS do share some common challenges, such as fast motion, and object occlusion. However, due to their specific application scenarios, many challenges are different. For instance, VOS may pay more attention to scenes that appear in human created media, which often have large camera motion, deformation, and appearance changes.

VSS instead often focuses on applications like autonomous driving, which requires a good trade off between accuracy and latency, accurate detection of small objects, model parallelization, and cross-domain generalization ability.

2.1.2 Inference Modes for Video Segmentation

VOS methods can be further classified into three types: automatic, semi-automatic, and interactive, according to how many human interventions are involved during inference.

- **Automatic Video Object Segmentation (AVOS).** AVOS, or *unsupervised video segmentation* or *zero-shot video segmentation*, performs VOS in an automatic manner, without any manual initialization (Fig. 1(a-b)). The input space \mathcal{X} refers to the video domain \mathcal{V} only. AVOS is suitable for video analysis but not for video editing that requires segmenting arbitrary objects or their parts flexibly; the typical application is virtual background creation in video conferencing.

- **Semi-automatic Video Object Segmentation (SVOS).** SVOS, also known as *semi-supervised video segmentation* or *one-shot video segmentation* [18], involves limited human inspection (typically provided in the first frame) to determine the desired objects (Fig. 1(c)). Thus for SVOS we have $\mathcal{X} = \mathcal{V} \times \mathcal{M}$, where \mathcal{V} indicates the video space and \mathcal{M} refers to human intervention. The most typical form of human intervention is first-frame object mask. In such case, SVOS is also called *pixel-wise tracking* or *mask propagation*. Some other forms of human input include bounding boxes and scribbles [8]. From this perspective, **language-guided video object segmentation (LVOS)** is a sub-branch of SVOS, where human intervention is given as linguistic descriptions about the desired objects, enabling efficient human-computer interaction (Fig. 1(e)). SVOS addresses AVOS techniques' lack of flexibility in defining target objects, but at the cost of additional human intervention. SVOS is typically applied in a user-friendly setting (without specialized equipment), such as video content creation in mobile phones. One of the core challenges in SVOS is how to fully utilize target information from limited human intervention.

- **Interactive Video Object Segmentation (IVOS).** SVOS models are designed to operate automatically once the target has been identified, while systems for IVOS incorporate user guidance throughout the analysis process (Fig. 1(d)). Thus IVOS can obtain high-quality segments and fits well for computer-generated imagery and video post-production, where tedious human supervision is possible. IVOS is also studied in the graphics community as *video cutout*. The input space \mathcal{X} for IVOS is $\mathcal{V} \times \mathcal{S}$, where \mathcal{S} typically refers to human scribbling. Key challenges include: 1) allowing users to easily specify segmentation constraints; 2) incorporating human specified constraints into the segmentation algorithm; 3) giving quick response to the constraints.

VSS methods typically work in an automatic mode (Fig. 1(f-h)), *i.e.*, $\mathcal{X} \equiv \mathcal{V}$; only a few early methods address the semi-automatic setting, called as *label propagation* [19].

Remark. The terms “unsupervised” and “semi-supervised” are conventionally used in VOS, to determine the amount of human interactions involved during inference. But they are easily confused with “unsupervised learning” and “semi-supervised learning”. We urge the community to replace the two fuzzy terms with “automatic” and “semi-automatic”.

2.1.3 Learning Paradigms for Video Segmentation

According to the learning strategy to approximate f^* , current deep learning-based video segmentation models can be grouped into three categories: supervised, unsupervised, and weakly supervised learning-based.

- **Supervised Learning-based Methods.** Modern video segmentation models are typically learned in a fully supervised manner, requiring N input training samples and their desired outputs $y_n := f^*(x_n)$, where $\{(x_n, y_n)\}_n \subset \mathcal{X} \times \mathcal{Y}$. The standard method for evaluating learning outcomes follows an *empirical risk/loss minimization* formulation¹:

$$\tilde{f} \in \arg \min_{f \in \mathcal{F}} \frac{1}{N} \sum_n \varepsilon(f(x_n), z(x_n)), \quad (1)$$

where \mathcal{F} denotes the hypothesis (solution) space, and $\varepsilon : \mathcal{X} \times \mathcal{Y} \mapsto \mathbb{R}$ is an error function that evaluates the estimate $f(x_n)$ against video segmentation related prior knowledge $z(x_n) \in \mathcal{Z}$. To make \tilde{f} a good approximation of f^* , current supervised video segmentation methods directly use the desired output y_n , *i.e.*, $z(x_n) := f^*(x_n)$, as the prior knowledge, with the price of requiring vast amounts of well-labeled data.

- **Unsupervised Learning-based Methods.** When only samples $\{x_n\}_n \subset \mathcal{X}$ are given, the problem of approximating f^* is known as unsupervised learning. The prior knowledge \mathcal{Z} , in such a setting, is typically built upon certain intrinsic properties of video data (*e.g.*, cross-frame consistency).

- **Weakly-Supervised Learning-based Methods.** In this case, \mathcal{Z} is typically a more easily-annotated domain, such as tags, bounding boxes, or scribbles. Then f^* is approximated using a finite number of samples from $\mathcal{X} \times \mathcal{Z}$.

Remark. So far, deep supervised learning-based methods are dominant in the field of video segmentation. However, exploring the task in an unsupervised or weakly supervised setting is more appealing, not only because it alleviates the annotation burden of \mathcal{Y} , but because it inspires an in-depth understanding of the nature of the task by exploring \mathcal{Z} .

2.2 History and Terminology

The history of segmentation of digital images using computers can be traced back 50 years [20]. In 1965, Roberts designed an operator for edge detection [20], representing the first step toward decomposing an image into its constitutive components. Since then, numerous algorithms for image segmentation have been proposed, and many are extended to the video domain. The field of video segmentation has evolved quickly and undergone great change.

Earlier attempts focus on **video over-segmentation**, *i.e.*, partitioning a video into space-time homogeneous, perceptually distinct-regions. Typical ones include hierarchical video segmentation [7], temporal superpixel [21], and supervoxels [3], based on the discontinuity and similarity of pixel intensities in a particular location, *i.e.*, separating pixels according to abrupt changes in intensity or grouping pixels with similar intensity together. They are instructive for early stage video preprocessing, but cannot solve the problem of object-level pattern modeling, as they do not provide any principled approach to flatten the hierarchical video decomposition into a binary segmentation [2], [9].

To extract foreground objects from video sequences, **background subtraction** techniques emerged beginning in

1. We omit the regularization term for brevity.

the late 70s [22], and became popular following the work of [23]. They assume that the background is known a priori, and that the camera is stationary [24], [25] or undergoes a predictable, parametric 2D [26] or 3D motion with 3D parallax [27], [28]. These geometry-based methods fit well for specific application scenarios such as surveillance systems [9], [25], but they are sensitive to model selection (2D or 3D), and cannot handle non-rigid camera movements. Another group of video segmentation solutions is introduced to tackle the task of **motion segmentation**, *i.e.*, finding objects in motion. Background subtraction can also be viewed as a specific case of motion segmentation. However, most motion segmentation models are built upon motion analysis [29], [30], factorization [31], and/or statistical [32] techniques, that comprehensively model the characteristics of moving scenes without prior knowledge of camera motion. Among the big family of motion segmentation algorithms, **trajectory segmentation** attained particular attention [4], [33]–[36]. Trajectories are generated through tracking points over multiple frames and have the advantage of representing long-term motion patterns, serving as an informative cue for segmentation. Though impressive, motion-based methods heavily rely on the accuracy of optical flow estimation and suffer difficulties when different parts of an object exhibit heterogeneous motions. To overcome these limitations, the task of extracting generic objects from unconstrained video sequences, *i.e.*, AVOS, drew more and more research interest [37]. Several methods [5], [38]–[40] explored object hypotheses, *i.e.*, object proposal [41], as middle-level object representations. They generated a large number of object candidates in every frame and cast the task of segmenting video objects as an object region selection problem. The main drawbacks of the proposal-based algorithms are the high computational cost [17] associated with proposal generation and complicated object inference schemes. Some others explored certain heuristic hypotheses, such as visual attention [1] and motion boundary [2], but they easily fail in scenarios where the heuristic assumptions do not hold.

As argued earlier, an alternative to above unattended solutions is to incorporate human-marked initialization, *i.e.*, SVOS. Older SVOS methods often rely on optical flow [8], [42]–[44] and share a similar spirit with *object tracking* [45], [46]. In addition, some pioneer IVOS methods were proposed to address high-quality video segmentation under extensive human guidance, including rotoscoping [47], [48], scribble [8], [49]–[52], contour [53] and point [54]. Significant engineering is typically needed to allow IVOS systems to operate at interactive speeds. In short, SVOS and IVOS pay for the improved flexibility and accuracy: they are unfeasible at large scale, due to the human-in-the-loop nature.

In the pre deep learning era, fewer efforts [12], [55], [56] were made at tackling VSS, due to greater complexity of the problem. These approaches typically relied on supervised classifiers such as SVMs and video over-segmentation techniques. There were also some weakly supervised solutions that learn VSS from tagged videos [57], [58].

Overall, traditional approaches for video segmentation, though giving interesting results, are constrained by hand-crafted features and heavy engineering. But deep learning brought the performance of video segmentation to a new level, as we will review in §3.

2.3 Related Research Area

There are several research fields closely related to video segmentation, which we now briefly describe.

- **Visual Tracking.** To infer the location of a target object over time, current tracking methods usually consider the situation where the target is determined by a bounding box in the first frame [59]. However, in more general tracking scenarios, and in particular the cases studied in early tracking methods, diverse object representations are explored [60], including centroids, skeletons, and contours. Some video segmentation techniques, such as background subtraction, are also merged into older trackers [61], [62]. Hence, visual tracking and video segmentation encounter some common challenges (*e.g.*, object/camera motion, appearance change, occlusion, *etc.*), fostering their mutual collaboration.

- **Image Semantic Segmentation.** The success of end-to-end image semantic segmentation [63] has sparked the rapid development of VSS. Rather than directly applying image semantic segmentation techniques frame by frame, recent VSS systems explore temporal continuity to increase both the accuracy and efficiency. Still, image semantic segmentation techniques will continue to serve as the foundation for the advance of its counterpart in the video domain.

- **Video Object Detection.** To generalize object detection in the video domain [64], video object detectors incorporate temporal cues over the box- or feature- level. There are many key technical steps/challenges, such as object proposal generation, temporal information aggregation, and cross-frame object association, that are shared between video object detection and (instance-level) video segmentation.

3 DEEP LEARNING-BASED VIDEO SEGMENTATION

3.1 Deep Learning-based VOS Models

VOS extracts generic foreground objects from video sequences with no concern for semantic category recognition. Based on how much human intervention is involved in inference, VOS models can be divided into three classes (§2.1.2): automatic (AVOS, §3.1.1), semi-automatic (SVOS, §3.1.2), and interactive (IVOS, §3.1.3). Moreover, although language-guided video object segmentation (LVOS) falls in the broader category of SVOS, LVOS methods are reviewed alone (§3.1.4), due to the specific multi-modal task setup.

3.1.1 Automatic Video Object Segmentation (AVOS)

Instead of using heuristic priors and hand-crafted features to automatically execute VOS, modern AVOS methods learn generic video object patterns in a data-driven fashion. We group landmark efforts based on their key techniques.

- **Deep Learning Module based Methods.** In 2015, Fragkiadaki *et al.* [108] made an early effort that learns a multi-layer perceptron to rank proposal segments and infer foreground objects. In 2016, Tsai *et al.* [43] proposed a joint optimization framework for AVOS and optical flow estimation with a naïve use of deep features from a pre-trained classification network. Later methods [69], [71] learn FCNs to predict initial, pixel-level foreground estimates from frame images [71], [109] or optical flow fields [69], while several post-processing steps are still needed. Basically, these primitive solutions largely rely on traditional AVOS techniques; the learning ability of neural networks is under-explored.

TABLE 1
Summary of essential characteristics for reviewed AVOS methods (§3.1.1).
Instance: instance- or object-level segmentation; **Flow:** if optical flow is used.

Year	Method	Pub.	Core Architecture	Instance	Flow	Training Dataset
2017	FSEG [65]	CVPR	Two-Stream FCN	Object	✓	ImageNet VID [66] + DAVIS ₁₆ [17]
	SFL [67]	ICCV	Two-Stream FCN	Object	✓	DAVIS ₁₆ [17]
	LVO [68]	ICCV	Two-Stream FCN	Object	✓	DAVIS ₁₆ [17]
	LMP [69]	ICCV	FCN	Object	✓	FT3D [70]
	NRF [71]	ICCV	FCN	Object	✓	Youtube-Objects [72]
2018	IST [73]	CVPR	FCN	Object	✓	DAVIS ₁₆ [17]
	FGRNE [74]	CVPR	FCN + RNN	Object	✓	SegTrackV2 [75] + DAVIS ₁₆ [17] + FBMS [36]
	MBN [76]	ECCV	FCN	Object	✓	DAVIS ₁₆ [17]
	PDB [77]	ECCV	RNN	Object	✓	DAVIS ₁₆ [17]
	MOT [78]	ICRA	Two-Stream FCN	Object	✓	DAVIS ₁₆ [17]
2019	RVOS [79]	CVPR	RNN	Instance	✓	DAVIS ₁₇ [80]/Youtube-VIS [81]
	COSNet [82]	CVPR	Siamese FCN + Co-attention	Object	✓	MSRA10K [83] + DUT [84] + DAVIS ₁₆ [17]
	UMOD [85]	CVPR	Adversarial Network	Object	✓	SegTrackV2 [75] + DAVIS ₁₆ [17] + FBMS [36]
	AGS [86]	CVPR	FCN	Object	✓	SegTrackV2 [75] + DAVIS ₁₆ [17] + DUT [84] + PASCAL-S [87]
	AGNN [88]	ICCV	FCN + GNN	Object	✓	MSRA10K [83] + DUT [84] + DAVIS ₁₆ [17]
	MGA [89]	ICCV	Two-Stream FCN	Object	✓	DUTS [90] + DAVIS ₁₆ [17] + FBMS [36]
	AnDiff [91]	ICCV	Siamese FCN + Co-attention	Object	✓	DAVIS ₁₆ [17]
LSMO [92]	IJCV	Two-Stream FCN	Object	✓	FT3D [70] + DAVIS ₁₆ [17]	
2020	MATNet [93]	AAAI	Two-Stream FCN	Object	✓	Youtube-VOS [94] + DAVIS ₁₆ [17]
	PyramidCSA [95]	AAAI	Siamese FCN + Co-attention	Object	✓	DUTS [90] + DAVIS ₁₆ [17] + DAVSOD [96]
	MuG [97]	CVPR	FCN	Object	✓	OxUvA [98]
	EGMN [99]	ECCV	FCN + Episodic Memory	Object	✓	MSRA10K [83] + DUT [84] + DAVIS ₁₆ [17]
	WCSNet [100]	ECCV	Siamese FCN	Object	✓	SALICON [101] + PASCAL VOC 2012 [102] + DUTS [90] + DAVIS ₁₆ [17]
	DFNet [103]	ECCV	Siamese FCN	Object	✓	MSRA10K [83] + DUT [84] + DAVIS ₁₆ [17]
2021	F2Net [104]	AAAI	Siamese FCN	Object	✓	MSRA10K [83] + DAVIS ₁₆ [17]
	TODA [105]	CVPR	Siamese FCN	Instance	✓	DAVIS ₁₇ [80]/Youtube-VIS [81]
	RTNet [106]	CVPR	Two-Stream FCN	Object	✓	DUTS [90] + DAVIS ₁₆ [17]
	DyStab [107]	CVPR	Adversarial Network	Object	✓	SegTrackV2 [75] + DAVIS ₁₆ [17] + FBMS [36]

• **Pixel Instance Embedding based Methods.** A group of AVOS models has been developed to make use of stronger deep learning descriptors [73], [76] – instance embeddings – learned from image instance segmentation data [110]. They first generate pixel-wise instance embeddings; the similarities between the embeddings measure whether the pixels belong to the same instance. Then, some representative embeddings are selected and clustered into foreground and background. The labels from these sampled embeddings are finally propagated to the other ones. The clustering and label propagation can be achieved without video specific supervision. Though using fewer annotations, these methods suffer from a fragmented and complicated pipeline.

• **End-to-end Methods with Short-term Information Encoding.** End-to-end model designs became the mainstream in this field. For example, convolutional recurrent neural networks (RNNs) were used to learn spatial and temporal visual patterns jointly [77], [88]. Another big family is built upon two-stream networks [65], [67], [68], [74], [89], [92], [93], wherein two parallel streams are built to extract features from raw image and optical flow, which are further fused for segmentation prediction. Two-stream methods make explicit use of appearance and motion cues, at the cost of optical flow computation and vast learnable parameters. These end-to-end methods improve accuracy and show the advantages of applying neural networks to this task. However, they only consider local content within very limited time span; they stack appearance and/or motion information from a few successive frames as input, ignoring relations among distant frames. Although RNNs are usually adopted, their internal hidden memory creates the inherent limits in modeling longer-term dependencies [111].

• **End-to-end Methods with Long-term Context Encoding.** Current leading AVOS models use global context over long time spans. In a seminal work [82], Lu *et al.* proposed a Siamese architecture-based AVOS model that extracts features for arbitrary frame pairs and captures cross-frame context by calculating pixel-wise feature correlations. During inference, for each test frame, context from several other frames (within the same video) is aggregated to locate pri-

mary objects. A contemporary work [91] exploited a similar idea but only used the first frame as reference for other test frames. Several papers [100], [106] based on [82] offered improvements such as making better use of information from multiple frames [88], [170], [171], encoding spatial context [104], and incorporating temporal consistency to improve representation power and computation efficiency [95], [103].

• **Un-/Weakly-supervised based Methods.** Only a handful of methods learn to perform AVOS from unlabeled or weakly labeled data. In [86], static image salient object segmentation and dynamic eye fixation data, which are more easily acquired compared with video segmentation data, are used to learn video generic object patterns. In [97], visual patterns are learned through exploring several intrinsic properties of video data at multiple granularities, *i.e.*, intra-frame saliency, short-term visual coherence, long-range semantic correspondence, and video-level discriminativeness. In [85], an adversarial contextual model is developed to segment moving objects without any manual annotation, achieved by minimizing the mutual information between the motions of an object and its context. This method is further enhanced in [107] by adopting a bootstrapping strategy and enforcing temporal consistency.

• **Instance-level AVOS Methods.** Instance-level AVOS, also referred as *multi-object unsupervised video segmentation*, was introduced with the launch of the DAVIS₁₉ challenge [172]. This task setting is more challenging as it requires not only separating the foreground objects from the background, but also discriminating different object instances. To tackle this task, current solutions typically work in a top-down fashion, *i.e.*, generating object candidates for each frames, and associating instances over different frames. In an early attempt [79], Ventura *et al.* delivered a recurrent network-based model that consists of a spatial LSTM for per-frame instance discovery and a temporal LSTM for cross-frame instance association. This method features an elegant model design, while its representation ability is too weak to enumerate all the object instances and to capture complex interactions between instances over the temporal domain. Thus later methods [170], [173], [174] strengthen the two-step

TABLE 2
Summary of essential characteristics for reviewed SVOS methods (§3.1.2). Flow: if optical flow is used.

Year	Method	Pub.	Core Architecture	Flow	Technical Feature	Training Dataset
2017	OSVOS [18]	CVPR	FCN		Online Fine-tuning	DAVIS ₁₆ [17]
	MaskTrack [112]	CVPR	FCN	✓	Propagation-based	ECSSD [113] + MSRA10K [83] + PASCAL-S [87] + DAVIS ₁₆ [17]
	CTN [114]	CVPR	FCN		Propagation-based	PASCAL VOC 2012 [102]
	VPN [115]	CVPR	Bilateral Network		Propagation-based	DAVIS ₁₆ [17]
	PLM [116]	CVPR	Siamese FCN		Matching-based	DAVIS ₁₆ [17]
	OnAVOS [117]	BMVC	FCN		Online Fine-tuning	PASCAL VOC 2012 [102] + COCO [118] + DAVIS [17]
	Lucid [119]	IJCV	Two-Stream FCN	✓	Propagation-based	DAVIS ₁₆ [17]
2018	CINM [120]	CVPR	Spatio-temporal MRF	✓	Propagation-based	DAVIS ₁₇ [80]
	FAVOS [121]	CVPR	FCN		Propagation-based	DAVIS ₁₆ [17]/DAVIS ₁₇ [80]
	RGMP [122]	CVPR	Siamese FCN		Propagation-based	PASCAL VOC 2012 [102] + ECSSD [113] + MSRA10K [83] + DAVIS ₁₇ [80]
	OSMN [123]	CVPR	FCN + Meta Learning		Online Fine-tuning	ImageNet VID [66] + DAVIS ₁₆ [17]
	MONet [124]	CVPR	FCN	✓	Online Fine-tuning	PASCAL VOC 2012 [102] + DAVIS ₁₆ [17]
	CRN [125]	CVPR	FCN + Active Contour	✓	Propagation-based	PASCAL VOC 2012 [102] + DAVIS ₁₆ [17]
	RCAL [126]	CVPR	FCN + RL		Propagation-based	MSRA10K [83] + PASCAL-S + SOD + ECSSD [113] + DAVIS ₁₆ [17]
	OSVOS-S [127]	PAMI	FCN		Online Fine-tuning	DAVIS ₁₆ [17]/DAVIS ₁₇ [80]
	Videomatch [128]	ECCV	Siamese FCN		Matching-based	DAVIS ₁₆ [17]/DAVIS ₁₇ [80]
	Dyenet [129]	ECCV	Re-ID		Propagation-based	DAVIS ₁₇ [80]
	LSE [130]	ECCV	FCN		Propagation-based	PASCAL VOC 2012 [102]
2019	Colorization [131]	ECCV	Siamese FCN		Unsupervised Learning	Kinetics [132]
	MVOS [133]	PAMI	Siamese FCN + Meta Learning		Online Fine-tuning	PASCAL VOC 2012 [102] + DAVIS ₁₆ [17]/DAVIS ₁₇ [80]
	FEELVOS [134]	CVPR	FCN		Matching-based	COCO [118] + DAVIS ₁₇ [80] + YouTube-VOS [94]
	MHP-VOS [135]	CVPR	Graph Optimization		Propagation-based	COCO [118] + DAVIS ₁₆ [17]/DAVIS ₁₇ [80]
	AGSS [136]	CVPR	FCN	✓	Propagation-based	DAVIS ₁₇ [80]/YouTube-VOS [94]
	AGAME [137]	CVPR	FCN		Propagation-based	MSRA10K [83] + PASCAL VOC 2012 [102] + DAVIS ₁₇ [80]/YouTube-VOS [94]
	StamMask [138]	CVPR	Siamese FCN		Box-Initialization	DAVIS ₁₆ [17]/DAVIS ₁₇ [80]/YouTube-VOS [94]
	RVOS [79]	CVPR	RNN		Propagation-based	DAVIS ₁₇ [80]/YouTube-VIS [81]
	BubbleNet [139]	CVPR	Siamese Network		Bubble Sorting	DAVIS ₁₇ [80]
	RANet [140]	ICCV	Siamese FCN		Matching-based	MSRA10K [83] + ECSSD [113] + HKU-IS [141] + DAVIS ₁₆ [17]/DAVIS ₁₇ [80]
	DMM-Net [142]	ICCV	Mask R-CNN		Differentiable Matching	DAVIS ₁₇ [80]/YouTube-VOS [94]
2020	DTN [143]	ICCV	FCN	✓	Propagation-based	COCO [118] + PASCAL VOC 2012 [102] + DAVIS ₁₆ /DAVIS ₁₇ [80]
	STM [144]	ICCV	Memory Network		Matching-based	PASCAL VOC 2012 [102] + COCO [118] + ECSSD [113] + DAVIS ₁₇ [80]/YouTube-VOS [94]
	TimeCycle [145]	ECCV	Siamese FCN		Unsupervised Learning	VLOG [146]
	UVC [147]	NeurIPS	Siamese FCN		Unsupervised Learning	COCO [118] + Kinetics [132]
	e-OSVOS [148]	NeurIPS	Mask R-CNN + Meta Learning		Online Fine-tuning	DAVIS ₁₇ [80] + YouTube-VOS [94]
	AFB-URR [149]	NeurIPS	Memory Network		Matching-based	PASCAL VOC 2012 [102] + COCO [118] + ECSSD [113] + DAVIS ₁₇ [80]/YouTube-VOS [94]
	Fasttan [150]	CVPR	Faster R-CNN		Propagation-based	COCO [118] + DAVIS ₁₇ [80]
	Fasttmu [151]	CVPR	FCN + RL		Box-Initialization	PASCAL VOC 2012 [102] + DAVIS ₁₇ [80]
	SAT [152]	CVPR	FCN + RL		Propagation-based	COCO [118] + DAVIS ₁₇ [80] + YouTube-VOS [94]
	FRIM-VOS [153]	CVPR	FCN		Matching-based	DAVIS ₁₇ [80]/YouTube-VOS [94]
	TVOS [154]	CVPR	FCN		Matching-based	DAVIS ₁₇ [80]/YouTube-VOS [94]
2021	MuG [97]	CVPR	Siamese FCN		Unsupervised Learning	OxUvA [98]
	MAST [155]	CVPR	Memory Network		Unsupervised Learning	OxUvA [98] + YouTube-VOS [94]
	GCNet [156]	ECCV	Memory Network		Matching-based	MSRA10K [83] + ECSSD [113] + HKU-IS [141] + DAVIS ₁₇ [80]/YouTube-VOS [94]
	KMN [157]	ECCV	Memory Network		Matching-based	PASCAL VOC 2012 [102] + COCO [118] + ECSSD [113] + DAVIS ₁₇ [80]/YouTube-VOS [94]
	CFB [158]	ECCV	FCN		Matching-based	COCO [118] + DAVIS ₁₇ [80]/YouTube-VOS [94]
	LWL [159]	ECCV	Siamese FCN + Meta Learning		Matching-based	DAVIS ₁₇ [80] + YouTube-VOS [94]
	MSN [160]	ECCV	Memory Network		Matching-based	DAVIS ₁₇ [80]/YouTube-VOS [94]
	EGMN [99]	ECCV	Memory Network		Matching-based	MSRA10K [83] + COCO [118] + DAVIS ₁₇ [80] + YouTube-VOS [94]
	STM-Cycle [161]	NeurIPS	Memory Network		Matching-based	DAVIS ₁₇ [80] + YouTube-VOS [94]
	QMA [162]	AAAI	Memory Network		Box-Initialization	DUT [84] + HKU-IS [141] + MSRA10K [83] + YouTube-VOS [94]
	SwiftNet [163]	CVPR	Memory Network		Matching-based	COCO [118] + DAVIS ₁₇ [80]/YouTube-VOS [94]
2021	G-FRTM [164]	CVPR	FCN + RL		Matching-based	DAVIS ₁₇ [80] + YouTube-VOS [94]
	SST [165]	CVPR	Transformer		Matching-based	DAVIS ₁₇ [80] + YouTube-VOS [94]
	GIEL [166]	CVPR	Siamese FCN		Matching-based	DAVIS ₁₇ [80] + YouTube-VOS [94]
	LCM [167]	CVPR	Memory Network		Matching-based	PASCAL VOC 2012 [102] + COCO [118] + ECSSD [113] + DAVIS ₁₇ [80]/YouTube-VOS [94]
	RMNet [168]	CVPR	Memory Network	✓	Matching-based	PASCAL VOC 2012 [102] + COCO [118] + ECSSD [113] + DAVIS ₁₇ [80]/YouTube-VOS [94]
	CRW [169]	NeurIPS	FCN		Unsupervised Learning	Kinetics [132]

pipeline through: i) employing image instance segmentation models (e.g., Mask R-CNN [175]) to detect an exhaustive set of object candidates, and ii) leveraging object tracking or re-identification techniques for instance association, supplemented by manually designed rules. Foreground/background AVOS techniques [82], [88] are also used to filter out nonsalient candidates [170], [174]. More recent methods [105] decompose the task into proposal generation and SVOS: object candidates are first generated, and corresponding tracklets are then obtained using advanced SVOS techniques. Overall, current instance-level AVOS models follow the classic tracking-by-detection paradigm, involving several ad-hoc designs. There is still considerable room for further improvement in accuracy and efficiency.

3.1.2 Semi-automatic Video Object Segmentation (SVOS)

Deep learning-based SVOS methods mainly focus on the first-frame *mask* propagation setting. They are categorized by their utilization of the test-time provided object masks.

• **Online Fine-tuning based Methods.** Following the one-shot principle, this family of methods [18], [124], [127], [133] trains a segmentation model separately on each given object mask in an online fashion. Fine-tuning methods essentially exploit the transfer learning capabilities of neural networks and often follow a two-step training procedure: i) *offline pre-training*: learn general segmentation features from images and video sequences, and ii) *online fine-tuning*: learn target-

specific representations from test-time supervision. The idea of fine-tuning was first introduced in [18], where only the initial image-mask pair is used for training an online, one-shot, but merely appearance-based FCN model. Then, in [117], more pixel samples in the unlabeled frames are mined as online training samples to better adapt to further changes over time. As [18], [117] have no notion of individual objects, [127] further incorporates instance segmentation models (e.g., Mask R-CNN [175]) during inference. While elegant through their simplicity, fine-tuning methods have several weaknesses: i) pre-training is fixed and not optimized for subsequent fine-tuning, ii) hyperparameters of online fine-tuning are often excessively hand-crafted and fail to generalize between test cases, iii) the common existing fine-tuning setups suffer from high test runtimes (up to 1,000 training iterations per segmented object online [18]). The root cause is that these approaches choose to encode all the target-related cues (i.e., appearance, mask) into network parameters implicitly. Towards efficient and automated fine-tuning, some recent methods [123], [133], [148] turn to meta learning techniques, i.e., optimize the fine-tuning policies [133], [148] (e.g., generic model initialization, learning rates, etc.) or even directly modify network weights [123].

• **Propagation-based Methods.** Two recent lines of research – built upon mask propagation and template matching techniques respectively – try to refrain from the online optimization to deliver compact, end-to-end SVOS solutions. In par-

ticular, propagation-based methods use the previous frame mask to infer the current frame mask [112], [114], [115]. For example, Jampani *et al.* [115] propose a bilateral network for long-range video-adaptive mask propagation. Perazzi *et al.* [112] approach SVOS by employing a modified FCN, where the previous frame mask is considered as an additional input channel. Follow-up work conducts optical flow guided mask alignment [124], performs heavy first-frame data augmentation [119], and adopts multi-step segmentation refinement [125]. Others use a re-identification module to retrieve missing objects after prolonged occlusions [129], design a reinforcement learning agent to conduct segmentation in a conditional decision-making process [126], or embed mask propagation into the inference of a spatiotemporal MRF model to improve temporal coherency [120]. Some researchers propose to learn location-aware embeddings to improve the discriminative ability of features [130], or to directly learn mask propagation through a sequence-to-sequence model [94]. Advanced tracking techniques are also exploited in [121], [135], [150], [152]. Propagation-based methods are found to easily suffer from error accumulation due to drifts and occlusions during mask propagation. Conditioning propagation on the initial frame-mask pair [122], [136], [143] seems a feasible solution to this. Although target-specific mask is explicitly encoded into the segmentation network, which makes up for the deficiencies of fine-tuning methods to a certain extent, propagation-based methods still learn object appearance by hidden network weights. Such implicit target-appearance modeling strategy hurts flexibility and adaptivity (although an exception is [137] which learns a generative model of target and background feature distributions to facilitate mask propagation).

- **Matching-based Methods.** Matching-based methods might possibly have been the most promising SVOS solution so far. This type of methods first constructs an embedding space to memorize the initial object embeddings, then classifies each pixel's label according to their similarities to the target object in the embedding space. Thus the initial object appearance is explicitly modeled, and no fine-tuning is necessary during inference. The earliest effort in this direction can be tracked back to [116]. Inspired by the advance in visual tracking [185], Yoon *et al.* [116] proposed a Siamese network to perform pixel-level matching between the first frame and upcoming frames. Later, [121] proposed to learn an embedding space from the first-frame supervision and pose VOS as a task of pixel retrieval: pixels are simply their respective nearest neighbors in the learned embedding space. The idea of [116] is also explored in [128], while it computes two matching maps for each upcoming frame, with respect to the foreground and background annotated in the first frame. In [134], pixel-level similarities computed from the first frame and from the previous frame are used as a guide to segment succeeding frames. Later, many matching-based solutions were proposed [140], [144], [186], perhaps most notably Oh *et al.*, who propose a space-time memory (STM) model to explicitly store previously computed segmentation information in an external memory [144]. The memory facilitates learning the evolution of objects over time and allows for comprehensive use of past segmentation cues even over long period of time. Almost all current top-leading SVOS solutions [154], [158] are built

upon STM; they improve the target adaption ability [99], [153], [159], incorporate local temporal continuity [157], [167], [168], explore instance-aware cues [166], and develop more efficient memory designs [149], [156], [160], [163]. Recently, [165] introduced a Transformer [187] based model, which performs matching-like computation through attending over a history of multiple frames. In general, matching-based solutions enjoy the advantage of flexible and differentiable model design as well as long-term correspondence modeling. On the other hand, feature matching relies on a powerful and generic feature embedding, which may limit its performance in challenging scenarios.

It is also worth mentioning that, as an effective technique for target-specific model learning, online learning is applied by many propagation [94], [112], [120], [125], [135] and matching [116], [129], [140] methods to boost performance.

- **Box-initialization based Methods.** As pixel-wise annotations are time-consuming or even impractical to acquire in realistic scenes, some work has considered the situation where the first-frame annotation is provided in the form of a bounding box. Specifically, in [138], Siamese trackers are augmented with a mask prediction branch. In [151], reinforcement learning is introduced to make decisions for target updating and matching. Later, in [162], an outside memory is utilized to build a stronger Siamese track-segmenter.

- **Un-/Weakly-supervised based Methods.** To alleviate the demand for large-scale, pixel-wise annotated training samples, several un-/weakly-supervised learning-based SVOS solutions were recently developed. They are typically built as a *reconstruction* scheme (*i.e.*, each pixel from a 'query' frame is reconstructed by finding and assembling related pixels from adjacent frame(s)) [131], [155], and/or adopt a *cycle-consistent tracking* paradigm (*i.e.*, pixels/patches are encouraged to fall into the same location after one cycle of forward and backward tracking) [97], [145], [147], [169].

- **Other Specific Methods.** Other papers make specific contributions that deserve a separate look. In [142], Zeng *et al.* extract mask proposals per frame and formulate the matching between object templates and proposals in a *differentiable* manner. Instead of using only the first frame annotation, [139] learns to select *the best frame* from the whole video for user interaction, so as to boost mask propagation. In [161], Li *et al.* introduce a forward-backward data flow based cycle consistency mechanism to improve both traditional SVOS training and offline inference protocols, through mitigating the error propagation problem. To accelerate processing speed, a dynamic network [164] is proposed to selectively allocate computation source for each frame, according to the similarity to the previous frame.

3.1.3 Interactive Video Object Segmentation (IVOS)

AVOS, without any human involvement, loses flexibility in segmenting arbitrary objects of user interest. SVOS additionally considers first-frame annotations, but easily fails in challenging scenes without human feedback. Moreover, the first-frame annotations are typically detailed masks, which are tedious to acquire: 79 seconds per instance for coarse polygon annotations of COCO [118], and much more for higher quality. Thus performing VOS in the interactive setting has gained increasing attention. Unlike classic models [48], [49], [52] requiring extensive and professional user

TABLE 3
Summary of essential characteristics for reviewed IVOS methods (§3.1.3).

Year	Method	Pub.	Core Architecture	Technical Feature	Training Dataset
2017	IIW [176]	-	FCN	Interaction-Propagation	PASCAL VOC 2012 [102]
2018	BFVOS [177]	CVPR	FCN	Pixel-wise Retrieval	DAVIS ₁₆ [17]
2019	IVS [178]	CVPR	FCN	Interaction-Propagation	DAVIS ₁₇ [80]+YouTube-VOS [94]
2020	MANet [179]	CVPR	Siamese FCN	Interaction-Propagation	DAVIS ₁₇ [80]
	ATNet [180]	ECCV	FCN	Interaction-Propagation	SBD + DAVIS ₁₇ [80]+YouTube-VOS [94]
	ScribbleBox [181]	ECCV	GCN	Interaction-Propagation	COCO [118] + ImageNet VID [66] + YouTube-VOS [94]
2021	IVOS-W [182]	CVPR	FCN + RL	Keyframe Selection	DAVIS ₁₇ [80]
	GIS [183]	CVPR	FCN	Interaction-Propagation	DAVIS ₁₇ [80]+YouTube-VOS [94]
	MiVOS [184]	CVPR	Memory Network	Interaction-Propagation	BL30K [184]+DAVIS ₁₇ [80] + YouTube-VOS [94]

TABLE 4
Summary of characteristics for reviewed LVOS methods (§3.1.4).

Year	Method	Pub.	Visual + Language Encoder	Technical Feature	Training Dataset
2018	A2DS [190]	CVPR	I3D + CNN	Dynamic Conv.	A2D Sentences [190]
	LangVOS [191]	ACCV	CNN + CNN	Cross-modal Att.	DAVIS ₁₇ -RVOS [190]
2019	AAN [192]	ICCV	I3D + CNN	Cross-modal Att.	A2D Sentences [190]
2020	CDNet [193]	AAAI	I3D + GRU	Dynamic Conv.	A2D Sentences [190]
	PolarRPE [194]	IJCAI	I3D + LSTM	Dynamic Conv.	A2D Sentences [190]
	VT-Capsule [195]	CVPR	I3D + CNN	Capsule Routing	A2D Sentences [190]
	URVOS [196]	ECCV	CNN + MLP	Cross-modal Att.	Refer-YouTube-VOS [196]
2021	CST [197]	CVPR	I3D + GRU	Cross-modal Att.	A2D Sentences [190]
	CMSANet [198]	PAMI	CNN + Word embed.	Cross-modal Att.	A2D Sentences [190]

intervention, recent deep learning-based IVOS solutions usually work with multiple rounds of scribble supervision, to minimize the user’s effort. In this scenario [188], the user draws scribbles on a selected frame and an algorithm computes the segmentation maps for all video frames in a batch process. For refinement, user intervention and segmentation are repeated. This *round-based interaction* [178] is useful for consumer-level applications and rapid prototyping for professional usage, where efficiency is the main concern. One can control the segmentation quality at the expense of time, as more rounds of interaction will provide better results.

- **Interaction-propagation based Methods.** The majority of current studies [183], [184] follow an *interaction-propagation* scheme. In the primary attempt [176], IVOS is achieved by a simple combination of two separate modules: an interactive image segmentation model [189] for producing and refining segmentation under user supervision; and a SVOS model [18] for propagating masks from the user-annotated frames to the others. Later, [178] devised a more compact solution, which also has two modules for interaction and propagation, respectively. However, the two modules are internally connected through intermediate feature exchanging, and also externally connected, *i.e.*, each of them is conditioned on the other’s output. In [180], a similar model design is also adopted, while the propagation part is equipped with two specific transfer modules for addressing local mask tracking (over adjacent frames) and global propagation (among distant frames), respectively. However, these techniques [176], [180] have to start a new feed-forward computation in each interaction round, making them inefficient as the number of rounds grows. A more efficient solution was developed in [179]. The critical idea is to build a common encoder for discriminative pixel embedding learning, upon which two small network branches are added for interactive segmentation and mask propagation, respectively. Thus the model extracts pixel embeddings for all frames only once (in the first round). In the following rounds, the feed-forward computation is only made within the two shallow branches.

- **Other Methods.** Chen *et al.* [177] propose a pixel embedding learning-based model, applicable to both SVOS and IVOS. With a similar idea of [121], IVOS is formulated as a pixel-wise retrieval problem, *i.e.*, transferring labels

to each pixel according to its nearest reference pixel. This model supports different kinds of user input, such as masks, clicks and scribbles, and can provide immediate feedback after user interaction. In [181], an interactive annotation tool is proposed for VOS. The annotation has two phases: annotating objects with tracked boxes, and labeling masks inside these tracks. Box tracks are annotated efficiently by approximating the trajectory using a parametric curve with a small number of control points which the annotator can interactively correct. Segmentation masks are corrected via scribbles which are propagated through time. In [182], a reinforcement learning framework is exploited to automatically determine the most valuable frame for interaction.

3.1.4 Language-guided Video Object Segmentation (LVOS)

LVOS is an emerging area, dating back to 2018 [190], [191]. Although there have already existed some efforts [239], [240] in the intersection of language and video understanding, none of them addresses pixel-level video-language reasoning. Most efforts in LVOS are made around the theme of efficient alignment between visual and linguistic modalities. According to the multi-modal information fusion strategy, existing models can be divided into three groups.

- **Dynamic Convolution-based Methods.** The first initiate was proposed in [190] that applies dynamic networks [241] for visual-language relation modeling. Specifically, convolution filters, dynamically generated from linguistic query, are used to adaptively transform visual features into desired segments. In the same line of work, [193], [194] incorporate spatial context into filter generation. However, as indicated by [192], linguistic variation of input description may greatly impact sentence representation and subsequently make dynamic filters unstable, causing inaccurate segmentation. For example, “car in blue is parked on the grass” and “blue car standing on the grass” have the same meaning but different generated filters, leading to poor performance.

- **Capsule Routing-based Methods.** In [195], both video and textual inputs are encoded through capsules [242], which are considered effective in modeling visual/textual entities. Then, dynamic routing is applied over the video and text capsules for visual-textual information integration.

- **Attention-based Methods.** Neural attention mechanism is also widely adopted in the field of LVOS [191], [196], [198], [243], due to its advantage in modeling global visual/textual context. In [192], two modules, called vision-guided language attention and language-guided vision attention, were developed to capture visual-textual correlations. In [197], two different attentions are learned to ground spatial- and temporal-content relevant linguistic cues to static and dynamic visual embeddings, respectively. In [243], multi-step, cross-modality attention-based reasoning is conducted.

TABLE 5
Summary of essential characteristics for reviewed VSS methods (§3.2). Flow: if optical flow is used.

Year	Method	Pub.	Seg. Level	Core Architecture	Flow	Technical Feature	Training Dataset
2016	Clockwork [199]	ECCV	Semantic	FCN	✓	Faster Segmentation	Cityscapes [200]/YouTube-Objects [72]
	FSO [201]	CVPR	Semantic	FCN + Dense CRF	✓	Temporal Feature Aggregation	Cityscapes [200]/CamVid [202]
	JFS [203]	ECCV	Semantic	FCN	✓	Temporal Feature Aggregation	KITTI MOTS [204]
2017	BANet [205]	CVPR	Semantic	FCN + LSTM	✓	Keyframe Selection	CamVid [202]/KITTI
	PEARL [206]	ICCV	Semantic	FCN	✓	Flow-guided Feature Aggregation	Cityscapes [200]/CamVid [202]
	NetWarp [207]	ICCV	Semantic	Siamese FCN	✓	Flow-guided Feature Aggregation	Cityscapes [200]/CamVid [202]
	DFE [208]	ICCV	Semantic	FCN	✓	Flow-guided Feature Aggregation	Cityscapes [200]
	BBF [209]	ICCV	Semantic	Two-Stream FCN	✓	Weakly-Supervised Learning	Cityscapes [200]/CamVid [202]
2018	GRFP [210]	CVPR	Semantic	FCN + GRU	✓	Temporal Feature Aggregation	Cityscapes [200]/CamVid [202]
	LVS [211]	CVPR	Semantic	FCN	✓	Keyframe Selection	Cityscapes [200]/CamVid [202]
	DVSN [212]	CVPR	Semantic	FCN+RL	✓	Keyframe Selection	Cityscapes [200]
	EUVS [213]	ECCV	Semantic	Bayesian CNN	✓	Flow-guided Feature Aggregation	CamVid [202]
	GCRF [214]	CVPR	Semantic	FCN+CRF	✓	Gaussian CRF	CamVid [202]
2019	Accel [215]	CVPR	Semantic	FCN	✓	Keyframe Selection	KITTI
	S5seg [216]	CVPR	Semantic	FCN	✓	Weakly-Supervised Learning	Cityscapes [200]/CamVid [202]
	MOTS [204]	CVPR	Instance	Mask R-CNN	✓	Tracking by Detection	KITTI MOTS [204]/MOTSChallenge [204]
	MaskTrack R-CNN [81]	ICCV	Instance	Mask R-CNN	✓	Tracking by Detection	YouTube-VIS [81]
2020	EFC [217]	AAAI	Semantic	FCN	✓	Temporal Feature Aggregation	Cityscapes [200]/CamVid [202]
	TDNet [218]	CVPR	Semantic	Memory Network	✓	Attention-based Feature Aggregation	Cityscapes [200]/CamVid [202]/NYUDv2 [219]
	MaskProp [220]	CVPR	Instance	Mask R-CNN	✓	Instance Feature Propagation	YouTube-VIS [81]
	VPS [221]	CVPR	Panoptic	Mask R-CNN	✓	Spatio-Temporal Feature Alignment	VIPER-VPS [221]/Cityscapes-VPS [221]
	MOTSN [222]	CVPR	Instance	Mask R-CNN	✓	Unsupervised Learning	KITTI MOTS [204]/BDD100K [223]
	MVAE [224]	CVPR	Instance	Mask R-CNN+VAE	✓	Variational Inference	KITTI MOTS [204]/YouTube-VIS [81]
	ETC [225]	ECCV	Semantic	FCN + KD	✓	Knowledge Distillation	Cityscapes [200]/CamVid [202]
	Sipmask [226]	ECCV	Instance	FCOS	✓	Single-Stage Segmentation	YouTube-VIS [81]
	STem-Seg [227]	ECCV	Instance	FCN	✓	Spatio-Temporal Embedding Learning	DAVIS ₁₇ [80]/YouTube-VIS [81]/KITTI-MOTS [204]
	Naive-Student [228]	ECCV	Semantic	FCN+KD	✓	Semi-Supervised Learning	Cityscapes [200]
2021	CompFeat [229]	AAAI	Instance	Mask R-CNN	✓	Spatio-Temporal Feature Alignment	YouTube-VIS [81]
	TraDeS [230]	CVPR	Instance	Siamese FCN	✓	Tracking by Detection	MOT/nuScenes/KITTI MOTS [204]/YouTube-VIS [81]
	SG-Net [231]	CVPR	Instance	FCOS	✓	Single-Stage Segmentation	YouTube-VIS [81]
	VisTR [232]	CVPR	Instance	Transformer	✓	Transformer-based Segmentation	YouTube-VIS [81]
	SSDE [233]	CVPR	Semantic	FCN	✓	Semi-Supervised Learning	Cityscapes [200]
	SiamTrack [234]	CVPR	Panoptic	Siamese FCN	✓	Supervised Contrastive Learning	VIPER-VPS [221]/Cityscapes-VPS [221]
	ViP-DeepLab [235]	CVPR	Panoptic	FCN	✓	Depth-Aware Panoptic Segmentation	Cityscapes-VPS [221]
	HRN [236]	CVPR	Instance	Mask R-CNN	✓	Weakly-Supervised Learning	YouTube-VIS [81]/Cityscapes [200]
	SemiTrack [237]	CVPR	Instance	SOLO	✓	Semi-Supervised Learning	YouTube-VIS [81]/Cityscapes [200]
	Propose-Reduce [238]	ICCV	Instance	Mask R-CNN	✓	Propose and Reduce	DAVIS ₁₇ [80]/YouTube-VIS [81]

3.2 Deep Learning-based VSS Models

Video semantic segmentation aims to group pixels with different semantics (e.g., category or instance membership), where different semantics result in different types of segmentation tasks, such as (instance-agnostic) video semantic segmentation (VSS, §3.2.1), video instance segmentation (VIS, §3.2.2) and video panoptic segmentation (VPS, §3.2.3).

3.2.1 (Instance-agnostic) Video Semantic Segmentation (VSS)

Extending the success of deep learning-based image semantic segmentation techniques to the video domain has become a research focus in computer vision recently. To achieve this, the most straightforward strategy is the naïve application of an image semantic segmentation model in a frame-by-frame manner. But this strategy completely ignores temporal continuity and coherence cues provided in videos. To make better use of temporal information, research efforts in this field are mainly made along two lines.

- **Efforts towards More Accurate Segmentation.** A major stream of methods exploits cross-frame relations to boost the prediction accuracy. They typically first apply the very same segmentation algorithms to each frame independently. Then they add extra modules on top, e.g., optical flow-guided feature aggregation [206], [207], [213], and sequential network based temporal information propagation [210], to gather multi-frame context and get better results. For example, in some pioneer work [201], [203], after performing static semantic segmentation for each frame individually, optical flow [203] or 3D CRF [201] based post processing is applied for gaining temporally consistent segments. Later, [214] jointly learns CNN-based per-frame segmentation and CRF-based spatio-temporal reasoning. In [207], features wrapped from previous frames with optical flow are combined with the current frame features for prediction. These

methods require additional feature aggregation modules, which increase the computational costs during the inference. Recently, [217] proposes to only incorporate flow-guided temporal consistency into the training phase, without bringing any extra inference cost. But its processing speed is still bounded to the adopted per-frame segmentation algorithms, as all features must be recomputed at each frame. For these methods, the utility in time-sensitive application areas, such as mobile and autonomous driving, is limited.

- **Efforts towards Faster Segmentation.** Yet another complementary line of work tries to leverage temporal information to accelerate computation. They approximate the expensive per-frame forward pass with cheaper alternatives, i.e., reusing the features in neighbouring frames. In [199], parts of segmentation networks are adaptively executed across frames, thus reducing the computation cost. Later methods use keyframes to avoid processing of each frame, and then propagate the outputs or the feature maps to other frames. For instance, [208] employs optical flow to warp the features between the keyframe and non-key frames. Adaptive keyframe selection is later exploited in [205], [212], further enhanced by adaptive feature propagation [211]. In [215], Jain *et al.* use a large, strong model to predict the keyframe and use a compact one in non-key frames. Keyframe-based methods have different computational loads between keyframes and non-key frames, causing high maximum latency and unbalanced occupation of computation resources that may decrease system efficiency [218]. Additionally, the spatial misalignment of other frames with respect to the keyframes is challenging to compensate for and often leads to different quantity results between keyframes and non-key frames. In [225], a temporal consistency guided knowledge distillation technique is proposed to train a compact network, which is applied to all frames. In [218], several

weight-sharing sub-networks are distributed over sequential frames, whose extracted shallow features are composed for final segmentation. This trend of methods indeed speeds up inference, but still with the cost of reduced accuracy.

- **Semi/Weakly-supervised based Methods.** Away from these main battlefields, some researchers made efforts to learn VSS under annotation efficient settings. In [209], classifier heatmaps are used to learn VSS from image tags only. [216], [228] use both labeled and unlabeled video frames to learn VSS. They propagate annotations from labeled frames to other unlabeled, neighboring frames [216], or alternatively train teacher and student networks with groundtruth annotations and iteratively generated pseudo labels [228].

3.2.2 Video Instance Segmentation (VIS)

In 2019, Yang *et al.* extended image instance segmentation to the video domain [81], which requires simultaneous detection, segmentation and tracking of instances in videos. This task is also known as *multi-object tracking and segmentation* (MOTS) [204]. Based on the patterns of generating instance sequences, existing frameworks can be roughly categorized into four paradigms: i) *track-detect*, ii) *clip-match*, iii) *propose-reduce*, iv) *segment-as-a-whole*. Track-detect methods detect and segment instances for each individual frame, followed by obtaining instance sequences with frame-by-frame tracking [81], [204], [222], [224], [226], [229]–[231], [244]. For example, in [81], [204], Mask R-CNN [175] is adapted for VIS/MOTS by adding a tracking branch for cross-frame instance association. Clip-match methods divide an entire video into multiple short overlapped clips, and obtain VIS results for each clip through mask propagation [220] or spatial-temporal embedding [227]. Final instance sequences are generated by matching and merging neighboring clips. Both of the two paradigms need two independent steps to generate a complete sequence. They both generate multiple incomplete sequences (*i.e.*, frames or clips) from a video, and merge (or complete) them by tracking/matching at the second stage. Intuitively, these paradigms are vulnerable to error accumulation in the process of merging sequences, especially when occlusion or fast motion exists. To address these limitations, a propose-reduce paradigm is proposed in [238]. It first samples several key frames and obtains instance sequences by propagating the instance segmentation results from each key frame to the entire video. Then, the redundant sequence proposals of the same instances are removed. This paradigm not only discards the step of merging incomplete sequences, but also achieves robust results considering multiple key frames. However, these three types of methods still need complex heuristic rules to associate instances and/or multiple steps to generate instance sequences. The segment-as-a-whole paradigm [232] is more elegant; it poses the task as a direct sequence prediction problem by using the Transformer [187].

Almost all VIS models are built upon fully supervised learning, while [236], [237] are the exceptions. Specifically, in [236], motion and temporal consistency cues are leveraged to generate pseudo-labels from tag labeled videos for weakly supervised VIS learning. In [237], a semi-supervised embedding learning approach is proposed to learn VIS from pixel-wise annotated images and unlabeled videos.

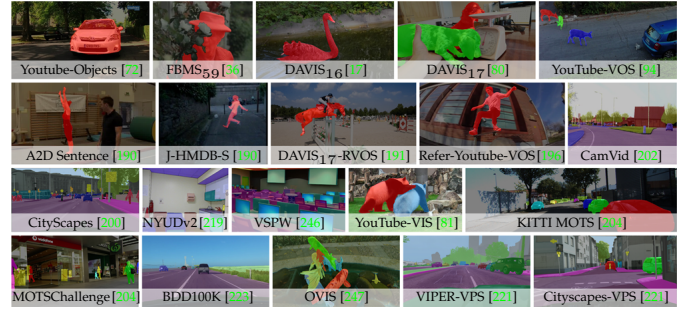


Fig. 3. Example frames from twenty famous video segmentation benchmark datasets. The ground-truth segmentation annotation is overlaid.

3.2.3 Video Panoptic Segmentation (VPS)

Very recently, Kim *et al.* extended image panoptic segmentation to the video domain [221], which aims at a holistic segmentation of all foreground instance tracklets and background regions, and assigning a semantic label to each video pixel. They adapt an image panoptic segmentation model [245] for VPS, by adding two modules for temporal feature fusion and cross-frame instance association, respectively. Later, temporal correspondence was explored in [234] through learning coarse segment-level and fine pixel-level matching. Qiao *et al.* [235] propose to learn monocular depth estimation and video panoptic segmentation jointly.

4 VIDEO SEGMENTATION DATASETS

Several datasets have been proposed for video segmentation over the past decades. Fig. 3 shows example frames from twenty commonly used datasets. We summarize their essential features in Table 6 and give detailed review below.

4.1 VOS Datasets

4.1.1 AVOS/SVOS/IVOS Datasets

- **Youtube-Objects** is a large dataset of 1,407 videos collected from 155 web videos belonging to 10 object categories (*e.g.*, dog, cat, plane, *etc.*). VOS models typically test the generalization ability on its subset [248], which has totally 126 shots with 20,647 frames, and provides coarse pixel-level fore-/background annotations on every 10^{th} frames.
- **FBMS₅₉** [36] consists of 59 video sequences with 13,860 frames in total. However, only 720 frames are annotated for fore-/background separation. The dataset is split into 29 and 30 sequences for training and evaluation, respectively.
- **DAVIS₁₆** [17] has 50 videos (30 for *train* set and 20 for *val* set) with 3,455 frames in total. For each frame, in addition to high-quality fore-/background segmentation annotation, a set of attributes (*e.g.*, deformation, occlusion, motion blur, *etc.*) are also provided to highlight the main challenges.
- **DAVIS₁₇** [80] contains 150 videos, *i.e.*, 60/30/30/30 videos for *train/val/test-dev/test-challenge* sets. Its *train* and *val* sets are extended from the respective sets in DAVIS₁₆. There are 10,459 frames in total. DAVIS₁₇ provides instance-level annotations to support SVOS. Then, DAVIS₁₈ challenge [188] provides scribble annotations to support IVOS. Moreover, as the original annotations of DAVIS₁₇ are biased towards the SVOS scenario, DAVIS₁₉ challenge [172] re-annotates *val* and *test-dev* sets of DAVIS₁₇ to support AVOS.
- **YouTube-VOS** [94] is a large-scale dataset, which is split into a *train* (3,471 videos), *val* (507 videos), and *test* (541 videos) set, in its newest 2019 version. Instance-level precise

TABLE 6
Statistics of representative video segmentation datasets. See §4.1 and §4.2 for more detailed descriptions.

Dataset	Year	Pub.	#Video	#Train/Val/Test/Dev	Annotation	Purpose	#Class	Synthetic
Youtube-Objects [72]	2012	CVPR	1,407 (126)	-/-/-/-	Object-level AVOS, SVOS	Generic	10	
FBMS ₅₉ [36]	2014	PAMI	59	29/30/-/-	Object-level AVOS, SVOS	Generic	-	
DAVIS ₁₆ [17]	2016	CVPR	50	30/20/-/-	Object-level AVOS, SVOS	Generic	-	
DAVIS ₁₇ [80]	2017	-	150	60/30/30/30	Instance-level AVOS, SVOS, IVOS	Generic	-	
YouTube-VOS [94]	2018	-	4,519	3,471/507/541/-	SVOS	Generic	94	
A2D Sentence [190]	2018	CVPR	3,782	3,017/737/-/-	RVOS	Human-centric	-	
J-HMDB Sentence [190]	2018	CVPR	928	-/-/-/-	RVOS	Human-centric	-	
DAVIS ₁₇ -RVOS [191]	2018	ACCV	90	60/30/-/-	RVOS	Generic	-	
Refer-Youtube-VOS [196]	2020	ECCV	3,975	3,471/507/-/-	RVOS	Generic	-	
CamVid [202]	2009	PRL	4	(frame: 467/100/233/-)	VSS	Urban	11	
CityScapes [200]	2016	CVPR	5,000	2,975/500/1,525	VSS	Urban	19	
NYUDv2 [219]	2012	ECCV	518	(frame: 795/654/-/-)	VSS	Indoor	40	
VSPW [246]	2021	CVPR	3,536	2,806/343/387/-	VSS	Generic	124	
YouTube-VIS [81]	2019	ICCV	3,859	2,985/421/453/-	VIS	Generic	40	
KITTI MOTS [204]	2019	CVPR	21	12/9/-/-	VIS	Urban	2	
MOTChallenge [204]	2019	CVPR	4	-/-/-/-	VIS	Urban	1	
BDD100K [223]	2020	ECCV	100,000	7,000/1,000/2,000/-	VSS, VIS	Driving	40 (VSS), 8 (VIS)	
OVIS [247]	2021	-	901	607/140/154/-	VIS	Generic	25	
VIPER-VPS [221]	2020	CVPR	124	(frame: 134K/50K/70K/-)	VPS	Urban	23	✓
Cityscapes-VPS [221]	2020	CVPR	500	400/100/-/-	VPS	Urban	19	

annotations are provided every five frames in a 30FPS frame rate. There are 94 object categories (*e.g.*, person, snake, *etc.*) in total, of which 26 are unseen in *train* set.

Remark. Youtube-Objects, FBMS₅₉ and DAVIS₁₆ are used for instance-agnostic AVOS and SVOS evaluation. DAVIS₁₇ is unique in comprehensive annotations for instance-level AVOS, SVOS as well as IVOS, but its scale is relatively small. YouTube-VOS is the largest one but only supports SVOS benchmarking. There also exist some other VOS datasets, such as SegTrack_{V1} [45] and SegTrack_{V2} [75], but they were less used recently, due to the limited scale and difficulty.

4.1.2 RVOS Datasets

- **A2D Sentence** [190] augments A2D [249] with phrases. It contains 3,782 videos, with 8 action classes performed by 7 actors. In each video, 3 to 5 frames are provided with segmentation masks. It contains 6,655 sentences describing actors and their actions. The dataset is split into 3,017/737 for *train/test*, and 28 unlabeled videos are ignored [192].
- **J-HMDB Sentence** [190] is built upon J-HMDB [250]. It is comprised of 928 short videos with 928 corresponding sentences describing 21 different action categories.
- **DAVIS₁₇-RVOS** [191] extends DAVIS₁₇ by collecting referring expressions for the annotated objects. 90 videos from *train* and *val* sets are annotated with more than 1,500 referring expressions. They provide two types of annotations, which describe the highlighted object: i) based on the entire video (*i.e.*, full-video expression) and ii) using only the first frame of the video (*i.e.*, first-frame expression).
- **Refer-Youtube-VOS** [196] includes 3,975 videos from YouTube-VOS [94], with 27,899 language descriptions of target objects. Similar to DAVIS₁₇-RVOS [191], both full-video and first-frame expression annotations are provided.

Remark. To date, A2D Sentence and J-HMDB Sentence are the main test-bed. However, the phrases are not produced with the aim of reference, but description, and limited to only a few object categories corresponding to the dominant ‘actors’ performing a salient ‘action’ [196]. But newly introduced DAVIS₁₇-RVOS and Refer-Youtube-VOS show improved difficulties in both visual and linguistic modalities.

4.2 VSS Datasets

- **CamVid** [202] is composed of 4 urban scene videos with 11-class pixelwise annotations. Each video is annotated ev-

ery 30 frames. The annotated frames are usually grouped into 467/100/233 for *train/val/test* [201].

- **CityScapes** [200] is a large-scale VSS dataset for street views. It has 2,975/500/1,525 snippets for *train/val/test*, captured at 17FPS. Each snippet contains 30 frames, and only the 20th frame is densely labelled with 19 semantic classes. 20,000 coarsely annotated frames are also provided.
- **NYUDv2** [219] contains 518 indoor RGB-D videos with high-quality ground-truths (every 10th video frame is labeled). There are 795 training frames and 654 testing frames being rectified and annotated with 40-class semantic labels.
- **VSPW** [246] is a recently proposed large-scale VSS dataset. It addresses video scene parsing in the wild by considering diverse scenarios. It consists of 3,536 videos, and provides pixel-level annotations for 124 categories at 15FPS. The *train/val/test* sets contain 2,806/343/387 videos with 198,244/24,502/28,887 frames, respectively.
- **YouTube-VIS** [81] is built upon YouTube-VOS [94] with instance-level annotations. Its newest 2021 version has 3,859 videos (2,985/421/453 for *train/val/test*) with 40 semantic categories. It provides 232K high-quality annotations for 8,171 unique video instances.
- **KITTI MOTS** [204] extends the 21 training sequences of KITTI tracking dataset [251] with VIS annotations – 12 for training and 9 for validation, respectively. The dataset contains 8,008 frames with a resolution of 375 × 1242, 26,899 annotated cars and 11,420 annotated pedestrians.
- **MOTChallenge** [204] annotates 4 of 7 training sequences of MOTChallenge₂₀₁₇ [252]. It has 2,862 frames with 26,894 annotated pedestrians and presents many occlusion cases.
- **BDD100K** [223] is a large-scale dataset with 100K driving videos (40 seconds and 30FPS each) and supports various tasks, including VSS and VIS. For VSS, 7,000/1,000/2,000 frames are densely labelled with 40 semantic classes for *train/val/test*. For VIS, 90 videos with 8 semantic categories are annotated by 129K instance masks – 60 training videos, 10 validation videos, and 20 testing videos.
- **OVIS** [247] is a new challenging VIS dataset, where object occlusions usually occur. It has 901 videos and 296K high-quality instance masks for 25 semantic categories. It is split into 607 training, 140 validation and 154 test videos.
- **VIPER-VPS** [221] re-organizes VIPER [253] into the video panoptic format. VIPER, extracted from the GTA-V game engine, has annotations of semantic and instance segmen-

TABLE 7

Quantitative object-level AVOS results on DAVIS₁₆ [17] val (§5.1.2) in terms of region similarity \mathcal{J} , boundary accuracy \mathcal{F} and time stability \mathcal{T} . We also report the recall and the decay performance over time for both \mathcal{J} and \mathcal{F} . (FPS denotes *frames per second*. The three best scores are marked in **red**, **blue**, and **green**, respectively. These notes also apply to the other tables.)

Method	\mathcal{J}			\mathcal{F}			\mathcal{T}	FPS \uparrow
	mean \uparrow	recall \uparrow	decay \downarrow	mean \uparrow	recall \uparrow	decay \downarrow		
SFL [67]	67.4	81.4	6.2	66.7	77.1	5.1	28.2	3.3
LVO [68]	75.9	89.1	0.0	72.1	83.4	1.3	26.5	13.5
LMP [69]	70.0	85.0	1.3	65.9	79.2	2.5	57.2	18.3
FSEG [65]	70.7	83.0	1.5	65.3	73.8	1.8	32.8	7.2
PDB [77]	77.2	93.1	0.9	74.5	84.4	-0.2	29.1	2.0
MOT [78]	77.2	87.8	5.0	77.4	84.4	3.3	27.9	1.0
LSMO [92]	78.2	91.1	4.1	75.9	84.7	3.5	21.2	>2.5
AGS [86]	79.7	89.1	1.9	77.4	85.8	0.0	26.7	1.7
COSNet [82]	80.5	93.1	4.4	79.4	89.5	5.0	18.4	2.2
AGNN [88]	81.3	93.1	0.0	79.7	88.5	5.1	33.7	1.9
AnDiff [91]	81.7	90.9	2.2	80.5	85.1	0.6	21.4	2.8
PyramidCSA [95]	78.1	90.1	-	78.5	88.2	-	-	11.0
MATNet [93]	82.4	94.5	5.5	80.7	90.2	4.5	21.6	1.3
EGMN [99]	82.5	94.3	4.2	81.2	90.3	5.6	19.8	5
DFNet [103]	83.4	-	-	81.8	-	-	15.9	3.6
F2Net [104]	83.1	95.7	0.0	84.4	92.3	0.8	20.9	10
RTNet [106]	85.6	96.1	-	84.7	93.8	-	-	6.7

tations for 10 thing and 13 stuff classes on 254K frames of ego-centric driving scenes at 1080 × 1920 resolution.

• **Cityscapes-VPS** [221] is built upon CityScapes [200]. Dense panoptic annotations for 8 thing and 11 stuff classes for 500 snippets in Cityscapes val set are provided every five frames and temporally consistent instance ids to the thing objects are also given, leading to 3000 annotated frames in total. These videos are split into 400/100 for train/val.

Remark. CamVid, CityScapes, NYUDv2, and VSPW are built for VSS benchmarking. YouTube-VIS, OVIS, KITTI MOTS, and MOTSChallenge are VIS datasets, but the diversity of the last two are limited. BDD100K has both VSS and VIS annotations. VIPER-VPS and Cityscapes-VPS are aware of VPS evaluation, but VIPER-VPS is a synthesized dataset.

5 PERFORMANCE COMPARISON

Next we tabulate the performance of previously discussed algorithms. For each of the reviewed fields, the most widely used dataset is selected for performance benchmarking². The performance scores and running speeds are gathered from the original articles, unless specified. It is essential to remark the difficulty when comparing runtime. As different methods are with different code bases and levels of optimization, it is hard to make fair runtime comparison [17], [63], [254]; the values are only provided for reference.

5.1 Object-level AVOS Performance Benchmarking

5.1.1 Evaluation Metrics

Presently, three metrics are frequently used [17] to measure how object-level AVOS methods perform on this task:

• **Region Jaccard** \mathcal{J} is calculated by the intersection-over-union (IoU) between the segmentation results $\hat{Y} \in \{0, 1\}^{w \times h}$ and the ground-truth $Y \in \{0, 1\}^{w \times h}$:

$$\mathcal{J} = \hat{Y} \cap Y / \hat{Y} \cup Y, \quad (2)$$

which computes the number of pixels of the intersection between \hat{Y} and Y , and divides it by the size of the union.

² For the methods reporting multiple scores due to the use of different training settings or backbone models, we adopt the best one.

TABLE 8

Quantitative instance-level AVOS results on DAVIS₁₇ [80] val (§5.2.2) in terms of region similarity \mathcal{J} and boundary accuracy \mathcal{F} .

Method	$\mathcal{J} \& \mathcal{F}$	\mathcal{J}			\mathcal{F}			FPS \uparrow
		mean \uparrow	recall \uparrow	decay \downarrow	mean \uparrow	recall \uparrow	decay \downarrow	
PDB [77]	55.1	53.2	58.9	4.9	57.0	60.2	6.8	0.7
RVOS [79]	41.2	36.8	40.2	0.5	45.7	46.4	1.7	14.3
AGS [86]	57.5	55.5	61.6	7.0	59.5	62.8	9.0	1.1
AGNN [170]	61.1	58.9	65.7	11.7	63.2	67.1	14.3	0.9
STEm-Seg [227]	64.7	61.5	70.4	-4.0	67.8	75.5	1.2	9.3
UnOVOST [173]	67.9	66.4	76.4	-0.2	69.3	76.9	0.0	1.0
TODA [105]	65.0	63.7	71.9	6.9	66.2	73.1	9.4	9.1

• **Boundary Accuracy** \mathcal{F} is the harmonic mean of the boundary precision P_c and recall R_c . The value of \mathcal{F} reflects how well the segment contours $c(\hat{Y})$ match the ground-truth contours $c(Y)$. Usually, the value of P_c and R_c can be computed via bipartite graph matching [255], then the boundary accuracy \mathcal{F} can be computed as:

$$\mathcal{F} = 2P_c R_c / (P_c + R_c). \quad (3)$$

• **Temporal Stability** \mathcal{T} is informative of the stability of segments. It is computed as the pixel-level cost of matching two successive segmentation boundaries. The match is achieved by minimizing the shape context descriptor [256] distances between matched points while preserving the order in which the points are present in the boundary polygon. Note that \mathcal{T} will compensate motion and small deformations, but not penalize the inaccuracies of the contours [17].

5.1.2 Results

We select DAVIS₁₆ [17], the most widely used dataset in AVOS, for performance benchmarking. Table 7 presents the results of those reviewed AVOS methods DAVIS₁₆ val set. The current best solution, RTNet [106], reaches 85.6 region similarity \mathcal{J} , significantly outperforming the earlier deep learning-based methods, such as SFL [67], proposed in 2017.

5.2 Instance-level AVOS Performance Benchmarking

5.2.1 Evaluation Metrics

In instance-level AVOS setting, region Jaccard \mathcal{J} , boundary accuracy \mathcal{F} , and $\mathcal{J} \& \mathcal{F}$ – the mean of \mathcal{J} and \mathcal{F} – are used for evaluation [172]. Each of the annotated object tracklets will be matched with one of predicted tracklets according to $\mathcal{J} \& \mathcal{F}$, using bipartite graph matching. For a certain criterion, the final score will be computed between each ground-truth object and its optimal assignment.

5.2.2 Results

Regarding instance-level AVOS, we take into account DAVIS₁₇ [80] in which the vast majority of methods are evaluated. From Table 8 we can find that UnOVOST [173] is the top scorer, with 67.9 \mathcal{J} at the time of this writing.

5.3 SVOS Performance Benchmarking

5.3.1 Evaluation Metrics

Region Jaccard \mathcal{J} , boundary accuracy \mathcal{F} , and $\mathcal{J} \& \mathcal{F}$ are also widely adopted for SVOS performance evaluation [188].

5.3.2 Results

DAVIS₁₇ [80] is also one of the most important SVOS dataset. Table 9 shows the results of recent SVOS methods on DAVIS₁₇ val set. In this case, all the top-leading solutions, such as EGMN [99], LCM [167], and RMNet [168], are built upon the memory augmented architecture – STM [144].

TABLE 10

Quantitative IVOS results on DAVIS₁₇ [80] val (§5.4.2) in terms of AUC and $\mathcal{J}@60$.

Method	AUC \uparrow	$\mathcal{J}@60$ \uparrow
IVS [178]	69.1	73.4
MA-Net [179]	74.9	76.1
ATNet [180]	77.1	79.0
GIS [183]	82.0	82.9
MiVOS [184]	84.9	85.4

TABLE 9

Quantitative SVOS results on DAVIS₁₇ [80] val (§5.3.2) in terms of region similarity \mathcal{J} and boundary accuracy \mathcal{F} .

Method	$\mathcal{J}\&\mathcal{F}$ mean \uparrow	\mathcal{J} mean \uparrow	\mathcal{F} mean \uparrow	FPS \uparrow	Method	$\mathcal{J}\&\mathcal{F}$ mean \uparrow	\mathcal{J} mean \uparrow	\mathcal{F} mean \uparrow	FPS \uparrow
OnAVOS [117]	67.9	64.5	70.5	0.08	STM [144]	81.8	79.2	84.3	6.3
OSVOS [18]	60.3	56.7	63.9	0.22	e-OSVOS [148]	77.2	74.4	80.0	0.5
CINM [120]	67.5	64.5	70.5	0.01	AFB-URR [149]	74.6	73.0	76.1	4
FAVOS [121]	58.2	54.6	61.8	0.56	Fasttan [150]	75.9	72.3	79.4	7
RGMP [122]	66.7	64.8	68.6	7.7	Fasttmu [151]	70.6	69.1	72.1	11
OSMN [123]	54.8	52.5	57.1	7.7	SAT [152]	72.3	68.6	76.0	39
OSVOS-S [127]	68.0	64.7	71.3	0.22	TVOS [154]	72.3	69.9	74.7	37
Videomatch [128]	61.4	-	-	0.38	GCNet [156]	71.4	69.3	73.5	25
Dyenet [129]	69.1	67.3	71.0	2.4	KMN [157]	76.0	74.2	77.8	8.3
MVOS [133]	59.2	56.3	62.1	1.5	CFBI [158]	81.9	79.3	84.5	2.2
FEELVOS [134]	71.5	69.1	74.0	2.2	LWL [159]	70.8	68.2	73.5	14
MHP-VOS [135]	75.3	71.8	78.8	0.01	MSN [160]	74.1	71.4	76.8	10
AGSS [136]	67.4	64.9	69.9	10	EGMN [99]	82.8	80.0	85.2	5
AGAME [137]	70.0	67.2	72.7	14	SwiftNet [163]	81.1	78.3	83.9	25
SiamMask [138]	56.4	64.3	58.5	35	G-FRTM [164]	76.4	-	-	18.2
RVOS [79]	60.6	57.5	63.6	0.56	SST [165]	82.5	79.9	85.1	-
RANet [140]	65.7	63.2	68.2	30	GIEL [166]	82.7	80.2	85.3	6.7
DMM-Net [142]	70.7	68.1	73.3	0.37	LCM [167]	83.5	80.5	86.5	8.5
DTN [143]	67.4	64.2	70.6	14.3	RMNet [168]	83.5	81.0	86.0	12

5.4 IVOS Performance Benchmarking

5.4.1 Evaluation Metrics

Area under the curve (AUC) and Jaccard at 60 seconds ($\mathcal{J}@60s$) are two widely used IVOS evaluation criteria [188].

- **AUC** is designed to measure the overall accuracy of the evaluation. It is computed over the plot Time *vs* Jaccard. Each sample in the plot is computed considering the average time and the average Jaccard for a certain interaction.
- **$\mathcal{J}@60$** measures the accuracy with a limited time budget (60 seconds). It is achieved by interpolating the Time *vs* Jaccard plot at 60 seconds. This evaluates which quality an IVOS method can obtain in 60 seconds.

5.4.2 Results

DAVIS₁₇ [80] is also widely used for IVOS performance benchmarking. Results summarized in Table 10 show that the method proposed by Cheng *et al.* [184] is the top one.

5.5 LVOS Performance Benchmarking

5.5.1 Evaluation Metrics

As suggested by [190], IoU and precision are used to assert the validity of LVOS methods.

- **IoU**: *overall IoU* and *mean IoU* are both computed; for former is computed as total intersection area of all test data over the total union area, while the latter refers to average over the IoU of each test sample. The *overall IoU* is biased toward large segmented regions, while *mean IoU* treats large and small regions equally.
- **Precision**: Precision@ K is computed as the percentage of testing samples whose IoU scores are higher than an overlap threshold K . Precision at five thresholds ranging from 0.5 to 0.9 as well as mean average precision (mAP) over 0.50:0.05:0.95 are reported.

TABLE 11

Quantitative LVOS results on A2D Sentence [190] test (§5.5.2) in terms of Precision@ K , mAP and IoU.

Method	Overlap					mAP \uparrow 0.5:0.95	IoU		FPS \uparrow
	P@0.5 \uparrow	P@0.6 \uparrow	P@0.7 \uparrow	P@0.8 \uparrow	P@0.9 \uparrow		overall \uparrow	mean \uparrow	
A2DS [190]	50.0	37.6	23.1	9.4	0.4	21.5	55.1	42.6	-
AAN [192]	55.7	45.9	31.9	16.0	2.0	27.4	60.1	49.0	8.6
VT-Capsule [195]	52.6	45.0	34.5	20.7	3.6	30.3	56.8	46.0	-
CDNet [193]	60.7	52.5	40.5	23.5	4.5	33.3	62.3	53.1	7.2
PolarRPE [194]	63.4	57.9	48.3	32.2	8.3	38.8	66.1	52.9	5.4
CST [197]	65.4	58.9	49.7	33.3	9.1	39.9	66.2	56.1	8.1

TABLE 12

Quantitative VSS results on Cityscapes [200] val (§5.6.2) in terms of IoU_{class} and IoU_{category} (Max Latency: maximum per-frame time cost).

Method	IoU _{class} \uparrow	IoU _{category} \uparrow	FPS \uparrow	Max Latency (ms) \downarrow
Clockwork [199]	66.4	88.6	6.4	198
DFP [208]	69.2	-	5.6	575
PEARL [206]	75.4	89.2	1.3	800
NetWarp [207]	80.5	91.0	-	-
DVSN [212]	70.3	-	19.8	-
LVS [211]	76.8	89.8	5.8	380
GRFP [210]	80.6	90.8	3.9	255
Accel [215]	75.5	-	1.1	-
VPLR [216]	81.4	-	5.9	-
TDNet [218]	79.9	-	5.6	178
EFC [217]	83.5	92.2	16.7	-
Lukas [233]	71.2	-	1.9	-

5.5.2 Results

A2D Sentence [190] is arguably the most popular dataset in LVOS. Table 11 gives the results of six recent methods on A2D Sentence test set. It shows clear improvement trend from the first LVOS model [190] proposed in 2018, to recent complicated solution developed by Hui *et al.* [197]. For runtime comparison, all the methods are tested on a video clip of 16 frames with resolution 512 \times 512 and a textual sequence of 20 words.

5.6 VSS Performance Benchmarking

5.6.1 Evaluation Metrics

IoU metric is the most widely used metric in VSS. Moreover, in Cityscapes [200] – the gold-standard benchmark dataset in this field, two IoU scores, IoU_{category} and IoU_{class}, defined over two semantic granularities, are reported. Here, ‘category’ refers to high-level semantic categories (*e.g.*, vehicle, human), while ‘class’ indicates more fine-grained semantic classes (*e.g.*, car, bicycle, person, rider). In total, [200] considers 19 classes, which are further grouped into 8 categories.

5.6.2 Results

Table 12 summarizes the results of eleven VSS approaches on Cityscapes [200] val set. As seen, EFC [217] performs the best currently, with 83.5% in terms of IoU_{class}.

5.7 VIS Performance Benchmarking

5.7.1 Evaluation Metrics

As in [81], precision and recall metrics are used for VIS performance evaluation. Precision at IoU thresholds 0.5 and 0.75, as well as mean average precision (mAP) over 0.50:0.05:0.95 are reported. Recall@ N is defined as the maximum recall given N segmented instances per video. These two metrics are first evaluated per category and then averaged over the category set. The IoU metric is similar to region Jaccard \mathcal{J} used in instance-level AVOS (§5.2.1).

TABLE 14
Quantitative VPS results on Cityscapes-VPS [221] (§5.8.2) $_{\text{test}}$ in term of VPQ. Each cell shows $\text{VPQ}^k / \text{VPQ}^k\text{-Thing} / \text{VPQ}^k\text{-Stuff}$.

Method	Temporal window size				VPQ \uparrow	FPS \uparrow
	$k = 0\uparrow$	$k = 5\uparrow$	$k = 10\uparrow$	$k = 15\uparrow$		
FuseTrack [221]	64.2 / 59.0 / 67.7	57.9 / 46.5 / 65.1	54.8 / 41.1 / 63.4	52.6 / 36.5 / 62.9	57.4 / 45.8 / 64.8	1.3
SiamTrack [234]	63.8 / 59.4 / 66.6	58.2 / 47.2 / 65.9	56.0 / 43.2 / 64.4	54.7 / 40.2 / 63.2	57.8 / 47.5 / 65.0	4.5
ViP-DeepLab [235]	68.9 / 61.6 / 73.5	62.9 / 51.0 / 70.5	59.9 / 46.0 / 68.8	58.2 / 42.1 / 68.4	62.5 / 50.2 / 70.3	10.0

TABLE 13
Quantitative VIS results on YouTube-VIS [81] the val (§5.7.2)
 in terms of Precision@ K , mAP, Recall@ N and IoU.

Method	P@0.5 \uparrow	P@0.75 \uparrow	R@1 \uparrow	R@10 \uparrow	mAP \uparrow 0.5:0.95	FPS \uparrow
MaskTrack R-CNN [81]	51.1	32.6	31.0	35.5	30.3	20
Sipmask [226]	53.0	33.3	33.5	38.9	32.5	24
STEm-Seg [227]	55.8	37.9	34.4	41.6	34.6	9
MaskProp [220]	-	45.6	-	-	42.5	1
CompFeat [229]	56.0	38.6	33.1	40.3	35.3	17
TraDeS [230]	52.6	32.8	29.1	36.6	32.6	26
SG-Net [231]	57.1	39.6	35.9	43.0	36.3	20
VisTR [232]	64.0	45.0	38.3	44.9	40.1	58
Propose-Reduce [238]	71.6	51.8	46.3	56.0	47.6	2

5.7.2 Results

Table 13 gathers VIS results for on YouTube-VIS [81] val set, showing that Transformer-based architecture, *i.e.*, VisTR [232], and redundant sequence proposal based solution Propose-Reduce [238], greatly improve the state-of-the-art.

5.8 VPS Performance Benchmarking

5.8.1 Evaluation Metrics

In [221], the panoptic quality (PQ) metric used in image panoptic segmentation is modified as video panoptic quality (VPQ) to adapt to video panoptic segmentation.

- **VPQ:** Given a snippet $V^{t:t+k}$ with time window k , true positive (TP) is defined by $\text{TP} = \{(u, \hat{u}) \in U \times \hat{U} : \text{IoU}(u, \hat{u}) > 0.5\}$ where U and \hat{U} are the set of the ground-truth and predicted tubes, respectively. False Positives (FP) and False Negatives (FN) are defined accordingly. After accumulating the TP_c , FP_c , and FN_c on all the clips with window size k and class c , VPQ is defined as:

$$\text{VPQ}^k = \frac{1}{N_{\text{class}}} \sum_c \frac{\sum_{(u, \hat{u}) \in \text{TP}_c} \text{IoU}(u, \hat{u})}{|\text{TP}_c| + \frac{1}{2}|\text{FP}_c| + \frac{1}{2}|\text{FN}_c|}. \quad (4)$$

When $k=1$, VPQ^1 is equivalent to PQ. For evaluation, VPQ^k is reported over different window sizes $k \in \{0, 5, 10, 15\}$ and the final VPQ is given as $\text{VPQ} = \frac{1}{4} \sum_{k \in \{0, 5, 10, 15\}} \text{VPQ}^k$.

5.8.2 Results

Cityscapes-VPS [221] is chosen for testing VPS methods. As shown in Table 14, ViP-DeepLab [235] is the top one.

5.9 Summary

From the results, we can draw several conclusions. The most important of them is related to reproducibility. Across different video segmentation areas, many methods do not describe the setup for the experimentation or do not provide the source code for implementation. Some of them even do not even release segmentation masks. Moreover, different methods use various datasets and backbone networks. These make fair comparison impossible and significantly hurt reproducibility.

Another important fact discovered thanks to this study is the lack of information about execution time and memory use. Many methods particularly in the fields of AVOS, LVOS, and VPS, do not report execution time and almost no paper reports memory use. This void is due to the fact that many methods focus only on accuracy without any concern about running time efficiency or memory requirements. However, in many application scenarios, such as mobile devices and self-driving cars, computational power and memory are typically limited. As benchmark datasets and challenges serve as a main driven factor behind the fast evolution of segmentation techniques, we encourage organizers of future video segmentation datasets to give this kind of metrics its deserved importance in benchmarking.

Finally, performance on some extensively studied video segmentation datasets, such as DAVIS₁₆ [17] in AVOS, DAVIS₁₇ [80] in SVOS, A2D Sentence [190] in LVOS, have nearly reached saturation. Though some new datasets are proposed recently and claim huge space for performance improvement, the dataset collectors just gather more challenging samples, without necessarily figuring out which exact challenges have and have not been solved.

6 FUTURE RESEARCH DIRECTIONS

Based on the reviewed research, we list several future research directions that we believe should be pursued.

- **Long-Term Video Segmentation:** Long-term video segmentation is much closer to practical applications, such as video editing. However, as the sequences in existing datasets often span several seconds, the performance of VOS models over long video sequences (*e.g.*, at the minute level) are still unexamined. Bringing VOS into the long-term setting will unlock new research lines, and put forward higher demand of the re-detection capability of VOS models.
- **Open World Video Segmentation:** Despite the obvious dynamic and open nature of the world, current VSS algorithms are typically developed in a closed-world paradigm, where all categories are known as a prior. These algorithms are often brittle once exposed to the realistic complexity of the open world, where they are unable to efficiently adapt and robustly generalize to unseen categories. For example, practical deployments of VSS systems in robotics, self-driving cars and surveillance cannot afford to have complete knowledge on what classes to expect at inference time, while being trained in-house. This calls for much smarter video segmentation systems, with a strong capability to identify unknown categories/instances in their environments [257].
- **Cooperation across Different Video Segmentation Sub-fields:** VOS and VSS, as the main branches of video segmentation, face many common challenges, *e.g.*, object occlusion, deformation, and fast motion. However, developments of the two fields are independent. Moreover, different VOS settings are related, while there are no precedents for modeling

these tasks in a unified framework. Thus we call for closer collaboration across different video segmentation sub-fields.

• **Annotation Efficient Video Segmentation Solutions:** Though great advances have been achieved in many videos segmentation tasks, current top algorithms are built on fully-supervised deep learning techniques, requiring a huge amount of annotated data. Though semi-supervised, weakly supervised and unsupervised alternatives were explored in some literature, annotation-efficient solutions receive far less attention and typically show weak performance, compared with the fully supervised ones. As the high temporal correlations in video data can provide additional cues for supervision, exploring existing annotation-efficient techniques in static semantic segmentation in the area of video segmentation is an appealing direction.

• **Learning Dense Spatiotemporal Features from Unlabeled Videos:** Recent years have witnessed the compelling success of unsupervised visual representation learning – with massive unlabeled data, meaningful visual representations can be learned and greatly improve the performance on down-stream tasks, such as image classification, even with limited labeled samples. This sheds light on potential directions for learning dense spatiotemporal features from unlabeled videos, or noisy web videos. The learned representations can be used to better initialize video segmentation networks and facilitate annotation efficient learning.

• **Adaptive Computation:** It is widely recognized that there exist high correlations among video frames. Though such data redundancy and continuity are exploited to reduce the computation cost in VSS, almost all current video segmentation models are fixed feed-forward structures or work alternatively between heavy and light-weight modes. We expect more flexible segmentation model designs towards more efficient and adaptive computation [258], which allows network architecture change on-the-fly – selectively activating part of the network in an input-dependent fashion.

• **Neural Architecture Search:** Video segmentation models are typically built upon hand-designed architectures, which may be suboptimal for capturing the nature of video data and limit the best possible performance. Using neural architecture search techniques to automate the design of video segmentation networks is a promising direction.

7 CONCLUSION

As far as we know, this is the first survey to comprehensively review recent progress in video segmentation, covering several sub-fields: AVOS, SVOS, IVOS, LVOS, VSS, VIS, and VPS. We provided the reader with the necessary background knowledge and summarized more than 150 deep learning models according to various criteria, including task settings, technique contributions, and learning strategies. We also presented a structured survey of 20 widely used video segmentation datasets and benchmarking results on 7 most widely-used ones. We discussed the results and provided insight into the shape of future research directions and open problems in the field. In conclusion, video segmentation has achieved notable progress thanks to the striking development of deep learning techniques, but several challenges still lie ahead. We expect this survey to provide an effective way to understand the current state-of-the-art and speed up the development of this research field.

REFERENCES

- [1] W. Wang, J. Shen, R. Yang, and F. Porikli, "Saliency-aware video object segmentation," *IEEE Trans. Pattern Anal. Mach. Intell.*, vol. 40, no. 1, pp. 20–33, 2017.
- [2] A. Papazoglou and V. Ferrari, "Fast object segmentation in unconstrained video," in *Proc. IEEE Int. Conf. Comput. Vis.*, 2013, pp. 1777–1784.
- [3] C. Xu and J. J. Corso, "Evaluation of super-voxel methods for early video processing," in *Proc. IEEE Conf. Comput. Vis. Pattern Recognit.*, 2012, pp. 1202–1209.
- [4] T. Brox and J. Malik, "Object segmentation by long term analysis of point trajectories," in *Proc. Eur. Conf. Comput. Vis.*, 2010, pp. 282–295.
- [5] Y. J. Lee, J. Kim, and K. Grauman, "Key-segments for video object segmentation," in *Proc. IEEE Int. Conf. Comput. Vis.*, 2011, pp. 1995–2002.
- [6] C.-P. Yu, H. Le, G. Zelinsky, and D. Samarasinghe, "Efficient video segmentation using parametric graph partitioning," in *Proc. IEEE Int. Conf. Comput. Vis.*, 2015, pp. 3155–3163.
- [7] M. Grundmann, V. Kwatra, M. Han, and I. Essa, "Efficient hierarchical graph-based video segmentation," in *Proc. IEEE Conf. Comput. Vis. Pattern Recognit.*, 2010, pp. 2141–2148.
- [8] N. Shankar Nagaraja, F. R. Schmidt, and T. Brox, "Video segmentation with just a few strokes," in *Proc. IEEE Int. Conf. Comput. Vis.*, 2015, pp. 3235–3243.
- [9] F. Perazzi, O. Wang, M. Gross, and A. Sorkine-Hornung, "Fully connected object proposals for video segmentation," in *Proc. IEEE Int. Conf. Comput. Vis.*, 2015, pp. 3227–3234.
- [10] V. Badrinarayanan, I. Budvytis, and R. Cipolla, "Semi-supervised video segmentation using tree structured graphical models," *IEEE Trans. Pattern Anal. Mach. Intell.*, vol. 35, no. 11, pp. 2751–2764, 2013.
- [11] W.-D. Jang and C.-S. Kim, "Streaming video segmentation via short-term hierarchical segmentation and frame-by-frame markov random field optimization," in *Proc. Eur. Conf. Comput. Vis.*, 2016, pp. 599–615.
- [12] B. Liu and X. He, "Multiclass semantic video segmentation with object-level active inference," in *Proc. IEEE Conf. Comput. Vis. Pattern Recognit.*, 2015, pp. 4286–4294.
- [13] J. Long, E. Shelhamer, and T. Darrell, "Fully convolutional networks for semantic segmentation," in *Proc. IEEE Conf. Comput. Vis. Pattern Recognit.*, 2015, pp. 3431–3440.
- [14] D. M. Thounaojam, A. Trivedi, K. M. Singh, and S. Roy, "A survey on video segmentation," in *Intelligent computing, networking, and informatics*, 2014, pp. 903–912.
- [15] Y.-J. Zhang, "An overview of image and video segmentation in the last 40 years," *Advances in Image and Video Segmentation*, pp. 1–16, 2006.
- [16] R. Yao, G. Lin, S. Xia, J. Zhao, and Y. Zhou, "Video object segmentation and tracking: A survey," *ACM Transactions on Intelligent Systems and Technology*, vol. 11, no. 4, pp. 1–47, 2020.
- [17] F. Perazzi, J. Pont-Tuset, B. McWilliams, L. Van Gool, M. Gross, and A. Sorkine-Hornung, "A benchmark dataset and evaluation methodology for video object segmentation," in *Proc. IEEE Conf. Comput. Vis. Pattern Recognit.*, 2016, pp. 724–732.
- [18] S. Caelles, K. Maninis, J. Pont-Tuset, L. Leal-Taixé, D. Cremers, and L. V. Gool, "One-shot video object segmentation," in *Proc. IEEE Conf. Comput. Vis. Pattern Recognit.*, 2017, pp. 5320–5329.
- [19] V. Badrinarayanan, F. Galasso, and R. Cipolla, "Label propagation in video sequences," in *Proc. IEEE Conf. Comput. Vis. Pattern Recognit.*, 2010, pp. 3265–3272.
- [20] L. G. Roberts, "Machine perception of three-dimensional solids," *Optical and Electro-Optical Information Processing*, 1965.
- [21] J. Chang, D. Wei, and J. W. Fisher, "A video representation using temporal superpixels," in *Proc. IEEE Conf. Comput. Vis. Pattern Recognit.*, 2013, pp. 2051–2058.
- [22] R. Jain and H.-H. Nagel, "On the analysis of accumulative difference pictures from image sequences of real world scenes," *IEEE Trans. Pattern Anal. Mach. Intell.*, no. 2, pp. 206–214, 1979.
- [23] C. R. Wren, A. Azarbayejani, T. Darrell, and A. P. Pentland, "Pfinder: Real-time tracking of the human body," *IEEE Trans. Pattern Anal. Mach. Intell.*, vol. 19, no. 7, pp. 780–785, 1997.
- [24] A. Criminisi, G. Cross, A. Blake, and V. Kolmogorov, "Bilayer segmentation of live video," in *Proc. IEEE Conf. Comput. Vis. Pattern Recognit.*, vol. 1, 2006, pp. 53–60.

- [25] S. Brutzer, B. Höferlin, and G. Heidemann, "Evaluation of background subtraction techniques for video surveillance," in *Proc. IEEE Conf. Comput. Vis. Pattern Recognit.*, 2011, pp. 1937–1944.
- [26] E. Hayman and J.-O. Eklundh, "Statistical background subtraction for a mobile observer," in *Proc. IEEE Int. Conf. Comput. Vis.*, vol. 2, 2003, pp. 67–67.
- [27] M. Irani and P. Anandan, "A unified approach to moving object detection in 2d and 3d scenes," *IEEE Trans. Pattern Anal. Mach. Intell.*, vol. 20, no. 6, pp. 577–589, 1998.
- [28] C. Yuan, G. Medioni, J. Kang, and I. Cohen, "Detecting motion regions in the presence of a strong parallax from a moving camera by multiview geometric constraints," *IEEE Trans. Pattern Anal. Mach. Intell.*, vol. 29, no. 9, pp. 1627–1641, 2007.
- [29] J. Y. Wang and E. H. Adelson, "Layered representation for motion analysis," in *Proc. IEEE Conf. Comput. Vis. Pattern Recognit.*, 1993, pp. 361–366.
- [30] H. S. Sawhney and S. Ayer, "Compact representations of videos through dominant and multiple motion estimation," *IEEE Trans. Pattern Anal. Mach. Intell.*, vol. 18, no. 8, pp. 814–830, 1996.
- [31] J. Costeira and T. Kanade, "A multi-body factorization method for motion analysis," in *Proc. IEEE Int. Conf. Comput. Vis.*, 1995, pp. 1071–1076.
- [32] D. Cremers and S. Soatto, "Motion competition: A variational approach to piecewise parametric motion segmentation," *International Journal of Computer Vision*, vol. 62, no. 3, pp. 249–265, 2005.
- [33] P. Ochs and T. Brox, "Object segmentation in video: A hierarchical variational approach for turning point trajectories into dense regions," in *Proc. IEEE Int. Conf. Comput. Vis.*, 2011, pp. 1583–1590.
- [34] K. Fragkiadaki, G. Zhang, and J. Shi, "Video segmentation by tracing discontinuities in a trajectory embedding," in *Proc. IEEE Conf. Comput. Vis. Pattern Recognit.*, 2012, pp. 1846–1853.
- [35] M. Keuper, B. Andres, and T. Brox, "Motion trajectory segmentation via minimum cost multicuts," in *Proc. IEEE Int. Conf. Comput. Vis.*, 2015, pp. 3271–3279.
- [36] P. Ochs, J. Malik, and T. Brox, "Segmentation of moving objects by long term video analysis," *IEEE Trans. Pattern Anal. Mach. Intell.*, vol. 36, no. 6, pp. 1187–1200, 2014.
- [37] A. Faktor and M. Irani, "Video segmentation by non-local consensus voting," in *Proceedings of the British Machine Vision Conference*, 2014.
- [38] T. Ma and L. J. Latecki, "Maximum weight cliques with mutex constraints for video object segmentation," in *Proc. IEEE Conf. Comput. Vis. Pattern Recognit.*, 2012, pp. 670–677.
- [39] D. Zhang, O. Javed, and M. Shah, "Video object segmentation through spatially accurate and temporally dense extraction of primary object regions," in *Proc. IEEE Conf. Comput. Vis. Pattern Recognit.*, 2013, pp. 628–635.
- [40] F. Xiao and Y. Jae Lee, "Track and segment: An iterative unsupervised approach for video object proposals," in *Proc. IEEE Conf. Comput. Vis. Pattern Recognit.*, 2016, pp. 933–942.
- [41] I. Endres and D. Hoiem, "Category independent object proposals," in *Proc. Eur. Conf. Comput. Vis.*, 2010, pp. 575–588.
- [42] S. Avinash Ramakanth and R. Venkatesh Babu, "SeamSeg: Video object segmentation using patch seams," in *Proc. IEEE Conf. Comput. Vis. Pattern Recognit.*, 2014, pp. 376–383.
- [43] Y.-H. Tsai, M.-H. Yang, and M. J. Black, "Video segmentation via object flow," in *Proc. IEEE Conf. Comput. Vis. Pattern Recognit.*, 2016, pp. 3899–3908.
- [44] W. Wang, J. Shen, F. Porikli, and R. Yang, "Semi-supervised video object segmentation with super-trajectories," *IEEE Trans. Pattern Anal. Mach. Intell.*, vol. 41, no. 4, pp. 985–998, 2018.
- [45] D. Tsai, M. Flagg, and J. M. Rehg, "Motion coherent tracking using multi-label MRF optimization," in *Proceedings of the British Machine Vision Conference*, 2010.
- [46] L. Wen, D. Du, Z. Lei, S. Z. Li, and M.-H. Yang, "JOTS: Joint online tracking and segmentation," in *Proc. IEEE Conf. Comput. Vis. Pattern Recognit.*, 2015, pp. 2226–2234.
- [47] A. Agarwala, A. Hertzmann, D. H. Salesin, and S. M. Seitz, "Keyframe-based tracking for rotoscoping and animation," *ACM Tran. Graphics*, vol. 23, no. 3, pp. 584–591, 2004.
- [48] W. Li, F. Viola, J. Starck, G. J. Brostow, and N. D. Campbell, "Roto++ accelerating professional rotoscoping using shape manifolds," *ACM Tran. Graphics*, vol. 35, no. 4, pp. 1–15, 2016.
- [49] X. Bai, J. Wang, D. Simons, and G. Sapiro, "Video SnapCut: robust video object cutout using localized classifiers," *ACM Tran. Graphics*, vol. 28, no. 3, p. 70, 2009.
- [50] A. Criminisi, T. Sharp, C. Rother, and P. Pérez, "Geodesic image and video editing," *ACM Tran. Graphics*, vol. 29, no. 5, pp. 134–1, 2010.
- [51] F. Zhong, X. Qin, Q. Peng, and X. Meng, "Discontinuity-aware video object cutout," *ACM Tran. Graphics*, vol. 31, no. 6, p. 175, 2012.
- [52] Q. Fan, F. Zhong, D. Lischinski, D. Cohen-Or, and B. Chen, "JumpCut: non-successive mask transfer and interpolation for video cutout," *ACM Tran. Graphics*, vol. 34, no. 6, pp. 195–1, 2015.
- [53] Y. Lu, X. Bai, L. Shapiro, and J. Wang, "Coherent parametric contours for interactive video object segmentation," in *Proc. IEEE Conf. Comput. Vis. Pattern Recognit.*, 2016, pp. 642–650.
- [54] W. Wang, J. Shen, and F. Porikli, "Selective video object cutout," *IEEE Trans. Image Process.*, vol. 26, no. 12, pp. 5645–5655, 2017.
- [55] A. Jain, S. Chatterjee, and R. Vidal, "Coarse-to-fine semantic video segmentation using supervoxel trees," in *Proc. IEEE Int. Conf. Comput. Vis.*, 2013, pp. 1865–1872.
- [56] A. Kae, B. Marlin, and E. Learned-Miller, "The shape-time random field for semantic video labeling," in *Proc. IEEE Conf. Comput. Vis. Pattern Recognit.*, 2014, pp. 272–279.
- [57] K. Tang, R. Sukthankar, J. Yagnik, and L. Fei-Fei, "Discriminative segment annotation in weakly labeled video," in *Proc. IEEE Conf. Comput. Vis. Pattern Recognit.*, 2013, pp. 2483–2490.
- [58] X. Liu, D. Tao, M. Song, Y. Ruan, C. Chen, and J. Bu, "Weakly supervised multiclass video segmentation," in *Proc. IEEE Conf. Comput. Vis. Pattern Recognit.*, 2014, pp. 57–64.
- [59] A. W. Smeulders, D. M. Chu, R. Cucchiara, S. Calderara, A. Dehghan, and M. Shah, "Visual tracking: An experimental survey," *IEEE Trans. Pattern Anal. Mach. Intell.*, vol. 36, no. 7, pp. 1442–1468, 2013.
- [60] A. Yilmaz, O. Javed, and M. Shah, "Object tracking: A survey," *ACM Computing Surveys*, vol. 38, no. 4, pp. 1–45, 2006.
- [61] C. Bibby and I. Reid, "Robust real-time visual tracking using pixel-wise posteriors," in *Proc. Eur. Conf. Comput. Vis.*, 2008, pp. 831–844.
- [62] X. Ren and J. Malik, "Tracking as repeated figure/ground segmentation," in *Proc. IEEE Conf. Comput. Vis. Pattern Recognit.*, 2007, pp. 1–8.
- [63] A. Garcia-Garcia, S. Orts-Escolano, S. Oprea, V. Villena-Martinez, P. Martinez-Gonzalez, and J. Garcia-Rodriguez, "A survey on deep learning techniques for image and video semantic segmentation," *Applied Soft Computing*, vol. 70, pp. 41–65, 2018.
- [64] L. Jiao, R. Zhang, F. Liu, S. Yang, B. Hou, L. Li, and X. Tang, "New generation deep learning for video object detection: A survey," *IEEE Trans. Neural Netw. Learning Sys.*, 2021.
- [65] S. D. Jain, B. Xiong, and K. Grauman, "Fusionseg: Learning to combine motion and appearance for fully automatic segmentation of generic objects in videos," in *Proc. IEEE Conf. Comput. Vis. Pattern Recognit.*, 2017, pp. 686–695.
- [66] O. Russakovsky, J. Deng, H. Su, J. Krause, S. Satheesh, S. Ma, Z. Huang, A. Karpathy, A. Khosla, M. Bernstein, A. C. Berg, and L. Fei-Fei, "ImageNet Large Scale Visual Recognition Challenge," *Int. J. Comput. Vis.*, vol. 115, no. 3, pp. 211–252, 2015.
- [67] J. Cheng, Y.-H. Tsai, S. Wang, and M.-H. Yang, "Segflow: Joint learning for video object segmentation and optical flow," in *Proc. IEEE Int. Conf. Comput. Vis.*, 2017, pp. 686–695.
- [68] P. Tokmakov, K. Alahari, and C. Schmid, "Learning video object segmentation with visual memory," in *Proc. IEEE Int. Conf. Comput. Vis.*, 2017, pp. 4491–4500.
- [69] —, "Learning motion patterns in videos," in *Proc. IEEE Conf. Comput. Vis. Pattern Recognit.*, 2017, pp. 531–539.
- [70] N. Mayer, E. Ilg, P. Hausser, P. Fischer, D. Cremers, A. Dosovitskiy, and T. Brox, "A large dataset to train convolutional networks for disparity, optical flow, and scene flow estimation," in *Proc. IEEE Conf. Comput. Vis. Pattern Recognit.*, 2016, pp. 4040–4048.
- [71] J. Li, A. Zheng, X. Chen, and B. Zhou, "Primary video object segmentation via complementary cnns and neighborhood reversible flow," in *Proc. IEEE Int. Conf. Comput. Vis.*, 2017, pp. 1417–1425.
- [72] A. Prest, C. Leistner, J. Civera, C. Schmid, and V. Ferrari, "Learning object class detectors from weakly annotated video," in *Proc. IEEE Conf. Comput. Vis. Pattern Recognit.*, 2012, pp. 3282–3289.
- [73] S. Li, B. Seybold, A. Vorobyov, A. Fathi, Q. Huang, and C.-C. Jay Kuo, "Instance embedding transfer to unsupervised video

- object segmentation," in *Proc. IEEE Conf. Comput. Vis. Pattern Recognit.*, 2018, pp. 6526–6535.
- [74] G. Li, Y. Xie, T. Wei, K. Wang, and L. Lin, "Flow guided recurrent neural encoder for video salient object detection," in *Proc. IEEE Conf. Comput. Vis. Pattern Recognit.*, 2018, pp. 3243–3252.
- [75] F. Li, T. Kim, A. Humayun, D. Tsai, and J. M. Rehg, "Video segmentation by tracking many figure-ground segments," in *Proc. IEEE Int. Conf. Comput. Vis.*, 2013, pp. 2192–2199.
- [76] S. Li, B. Seybold, A. Vorobyov, X. Lei, and C.-C. Jay Kuo, "Unsupervised video object segmentation with motion-based bilateral networks," in *Proc. Eur. Conf. Comput. Vis.*, 2018, pp. 215–231.
- [77] H. Song, W. Wang, S. Zhao, J. Shen, and K.-M. Lam, "Pyramid dilated deeper convlstm for video salient object detection," in *Proc. Eur. Conf. Comput. Vis.*, 2018, pp. 744–760.
- [78] M. Siam, C. Jiang, S. Lu, L. Petrich, M. Gamal, M. Elhoseiny, and M. Jagersand, "Video segmentation using teacher-student adaptation in a human robot interaction (hri) setting," in *International Conference on Robotics and Automation*, 2019, pp. 50–56.
- [79] C. Ventura, M. Bellver, A. Girbau, A. Salvador, F. Marques, and X. Giro-i Nieto, "Rvos: End-to-end recurrent network for video object segmentation," in *Proc. IEEE Conf. Comput. Vis. Pattern Recognit.*, 2019, pp. 5277–5286.
- [80] J. Pont-Tuset, F. Perazzi, S. Caelles, P. Arbeláez, A. Sorkine-Hornung, and L. Van Gool, "The 2017 davis challenge on video object segmentation," *arXiv preprint arXiv:1704.00675*, 2017.
- [81] L. Yang, Y. Fan, and N. Xu, "Video instance segmentation," in *Proc. IEEE Int. Conf. Comput. Vis.*, 2019, pp. 5188–5197.
- [82] X. Lu, W. Wang, C. Ma, J. Shen, L. Shao, and F. Porikli, "See more, know more: Unsupervised video object segmentation with co-attention siamese networks," in *Proc. IEEE Conf. Comput. Vis. Pattern Recognit.*, 2019, pp. 3623–3632.
- [83] M.-M. Cheng, N. J. Mitra, X. Huang, P. H. Torr, and S.-M. Hu, "Global contrast based salient region detection," *IEEE Trans. Pattern Anal. Mach. Intell.*, vol. 37, no. 3, pp. 569–582, 2015.
- [84] C. Yang, L. Zhang, H. Lu, X. Ruan, and M. Yang, "Saliency detection via graph-based manifold ranking," in *Proc. IEEE Conf. Comput. Vis. Pattern Recognit.*, 2013, pp. 3166–3173.
- [85] Y. Yang, A. Loquercio, D. Scaramuzza, and S. Soatto, "Unsupervised moving object detection via contextual information separation," in *Proc. IEEE Conf. Comput. Vis. Pattern Recognit.*, 2019, pp. 879–888.
- [86] W. Wang, H. Song, S. Zhao, J. Shen, S. Zhao, S. C. Hoi, and H. Ling, "Learning unsupervised video object segmentation through visual attention," in *Proc. IEEE Conf. Comput. Vis. Pattern Recognit.*, 2019, pp. 3064–3074.
- [87] Y. Li, X. Hou, C. Koch, J. M. Rehg, and A. L. Yuille, "The secrets of salient object segmentation," in *Proc. IEEE Conf. Comput. Vis. Pattern Recognit.*, 2014, pp. 280–287.
- [88] W. Wang, X. Lu, J. Shen, D. J. Crandall, and L. Shao, "Zero-shot video object segmentation via attentive graph neural networks," in *Proc. IEEE Int. Conf. Comput. Vis.*, 2019, pp. 9236–9245.
- [89] H. Li, G. Chen, G. Li, and Y. Yu, "Motion guided attention for video salient object detection," in *Proc. IEEE Int. Conf. Comput. Vis.*, 2019, pp. 7274–7283.
- [90] L. Wang, H. Lu, Y. Wang, M. Feng, D. Wang, B. Yin, and X. Ruan, "Learning to detect salient objects with image-level supervision," in *Proc. IEEE Conf. Comput. Vis. Pattern Recognit.*, 2017, pp. 136–145.
- [91] Z. Yang, Q. Wang, L. Bertinetto, W. Hu, S. Bai, and P. H. Torr, "Anchor diffusion for unsupervised video object segmentation," in *Proc. IEEE Int. Conf. Comput. Vis.*, 2019, pp. 931–940.
- [92] P. Tokmakov, C. Schmid, and K. Alahari, "Learning to segment moving objects," *Int. J. Comput. Vis.*, vol. 127, no. 3, pp. 282–301, 2019.
- [93] T. Zhou, S. Wang, Y. Zhou, Y. Yao, J. Li, and L. Shao, "Motion-attentive transition for zero-shot video object segmentation," in *AAAI Conference on Artificial Intelligence*, 2020, pp. 13 066–13 073.
- [94] N. Xu, L. Yang, Y. Fan, D. Yue, Y. Liang, J. Yang, and T. Huang, "Youtube-vos: A large-scale video object segmentation benchmark," *arXiv preprint arXiv:1809.03327*, 2018.
- [95] Y. Gu, L. Wang, Z. Wang, Y. Liu, M.-M. Cheng, and S.-P. Lu, "Pyramid constrained self-attention network for fast video salient object detection," in *AAAI Conference on Artificial Intelligence*, 2020, pp. 10 869–10 876.
- [96] D.-P. Fan, W. Wang, M.-M. Cheng, and J. Shen, "Shifting more attention to video salient object detection," in *Proc. IEEE Conf. Comput. Vis. Pattern Recognit.*, 2019, pp. 8554–8564.
- [97] X. Lu, W. Wang, J. Shen, Y.-W. Tai, D. J. Crandall, and S. C. Hoi, "Learning video object segmentation from unlabeled videos," in *Proc. IEEE Conf. Comput. Vis. Pattern Recognit.*, 2020, pp. 8960–8970.
- [98] J. Valmadre, L. Bertinetto, J. F. Henriques, R. Tao, A. Vedaldi, A. W. Smeulders, P. H. Torr, and E. Gavves, "Long-term tracking in the wild: A benchmark," in *Proc. Eur. Conf. Comput. Vis.*, 2018, pp. 670–685.
- [99] X. Lu, W. Wang, M. Danelljan, T. Zhou, J. Shen, and L. Van Gool, "Video object segmentation with episodic graph memory networks," in *Proc. Eur. Conf. Comput. Vis.*, 2020.
- [100] L. Zhang, J. Zhang, Z. Lin, R. Mech, H. Lu, and Y. He, "Unsupervised video object segmentation with joint hotspot tracking," in *Proc. Eur. Conf. Comput. Vis.*, 2020.
- [101] M. Jiang, S. Huang, J. Duan, and Q. Zhao, "Salicon: Saliency in context," in *Proc. IEEE Conf. Comput. Vis. Pattern Recognit.*, 2015, pp. 1072–1080.
- [102] M. Everingham, S. M. A. Eslami, L. J. V. Gool, C. K. I. Williams, J. M. Winn, and A. Zisserman, "The pascal visual object classes challenge: A retrospective," *Int. J. Comput. Vis.*, vol. 111, no. 1, pp. 98–136, 2015.
- [103] M. Zhen, S. Li, L. Zhou, J. Shang, H. Feng, T. Fang, and L. Quan, "Learning discriminative feature with crf for unsupervised video object segmentation," in *Proc. Eur. Conf. Comput. Vis.*, 2020, pp. 445–462.
- [104] D. Liu, D. Yu, C. Wang, and P. Zhou, "F2net: Learning to focus on the foreground for unsupervised video object segmentation," in *AAAI Conference on Artificial Intelligence*, 2021.
- [105] T. Zhou, J. Li, X. Li, and L. Shao, "Target-aware object discovery and association for unsupervised video multi-object segmentation," in *Proc. IEEE Conf. Comput. Vis. Pattern Recognit.*, 2021.
- [106] S. Ren, W. Liu, Y. Liu, H. Chen, G. Han, and S. He, "Reciprocal transformations for unsupervised video object segmentation," in *Proc. IEEE Conf. Comput. Vis. Pattern Recognit.*, 2021, pp. 15 455–15 464.
- [107] Y. Yang, B. Lai, and S. Soatto, "Dystab: Unsupervised object segmentation via dynamic-static bootstrapping," in *Proc. IEEE Conf. Comput. Vis. Pattern Recognit.*, 2021, pp. 2826–2836.
- [108] K. Fragkiadaki, P. Arbeláez, P. Felsen, and J. Malik, "Learning to segment moving objects in videos," in *Proc. IEEE Conf. Comput. Vis. Pattern Recognit.*, 2015, pp. 4083–4090.
- [109] W. Wang, J. Shen, and L. Shao, "Video salient object detection via fully convolutional networks," *IEEE Trans. Image Process.*, vol. 27, no. 1, pp. 38–49, 2017.
- [110] A. Fathi, Z. Wojna, V. Rathod, P. Wang, H. O. Song, S. Guadarrama, and K. P. Murphy, "Semantic instance segmentation via deep metric learning," *arXiv preprint arXiv:1703.10277*, 2017.
- [111] S. Sukhbaatar, A. Szlam, J. Weston, and R. Fergus, "End-to-end memory networks," in *Proc. Advances Neural Inf. Process. Syst.*, 2015, pp. 2440–2448.
- [112] F. Perazzi, A. Khoreva, R. Benenson, B. Schiele, and A. Sorkine-Hornung, "Learning video object segmentation from static images," in *Proc. IEEE Conf. Comput. Vis. Pattern Recognit.*, 2017, pp. 3491–3500.
- [113] Q. Yan, L. Xu, J. Shi, and J. Jia, "Hierarchical saliency detection," in *Proc. IEEE Conf. Comput. Vis. Pattern Recognit.*, 2013, pp. 1155–1162.
- [114] W.-D. Jang and C.-S. Kim, "Online video object segmentation via convolutional trident network," in *Proc. IEEE Conf. Comput. Vis. Pattern Recognit.*, 2017, pp. 5849–5858.
- [115] V. Jampani, R. Gadde, and P. V. Gehler, "Video propagation networks," in *Proc. IEEE Conf. Comput. Vis. Pattern Recognit.*, 2017, pp. 3154–3164.
- [116] J. S. Yoon, F. Rameau, J. Kim, S. Lee, S. Shin, and I. S. Kweon, "Pixel-level matching for video object segmentation using convolutional neural networks," in *Proc. IEEE Int. Conf. Comput. Vis.*, 2017, pp. 2186–2195.
- [117] P. Voigtlaender and B. Leibe, "Online adaptation of convolutional neural networks for video object segmentation," in *Proceedings of the British Machine Vision Conference*, 2017.
- [118] T.-Y. Lin, M. Maire, S. Belongie, J. Hays, P. Perona, D. Ramanan, P. Dollár, and C. L. Zitnick, "Microsoft coco: Common objects in context," in *Proc. Eur. Conf. Comput. Vis.*, 2014, pp. 740–755.
- [119] A. Khoreva, R. Benenson, E. Ilg, T. Brox, and B. Schiele, "Lucid data dreaming for video object segmentation," *International Journal of Computer Vision*, vol. 127, no. 9, pp. 1175–1197, 2019.

- [120] L. Bao, B. Wu, and W. Liu, "CNN in MRF: Video object segmentation via inference in a CNN-based higher-order spatio-temporal MRF," in *Proc. IEEE Conf. Comput. Vis. Pattern Recognit.*, 2018, pp. 5977–5986.
- [121] J. Cheng, Y.-H. Tsai, W.-C. Hung, S. Wang, and M.-H. Yang, "Fast and accurate online video object segmentation via tracking parts," in *Proc. IEEE Conf. Comput. Vis. Pattern Recognit.*, 2018, pp. 7415–7424.
- [122] S. Wug Oh, J.-Y. Lee, K. Sunkavalli, and S. Joo Kim, "Fast video object segmentation by reference-guided mask propagation," in *Proc. IEEE Conf. Comput. Vis. Pattern Recognit.*, 2018, pp. 7376–7385.
- [123] L. Yang, Y. Wang, X. Xiong, J. Yang, and A. K. Katsaggelos, "Efficient video object segmentation via network modulation," in *Proc. IEEE Conf. Comput. Vis. Pattern Recognit.*, 2018, pp. 6499–6507.
- [124] H. Xiao, J. Feng, G. Lin, Y. Liu, and M. Zhang, "Monet: Deep motion exploitation for video object segmentation," in *Proc. IEEE Conf. Comput. Vis. Pattern Recognit.*, 2018, pp. 1140–1148.
- [125] P. Hu, G. Wang, X. Kong, J. Kuen, and Y.-P. Tan, "Motion-guided cascaded refinement network for video object segmentation," in *Proc. IEEE Conf. Comput. Vis. Pattern Recognit.*, 2018, pp. 1400–1409.
- [126] J. Han, L. Yang, D. Zhang, X. Chang, and X. Liang, "Reinforcement cutting-agent learning for video object segmentation," in *Proc. IEEE Conf. Comput. Vis. Pattern Recognit.*, 2018, pp. 9080–9089.
- [127] K.-K. Maninis, S. Caelles, Y. Chen, J. Pont-Tuset, L. Leal-Taixé, D. Cremers, and L. Van Gool, "Video object segmentation without temporal information," *IEEE Trans. Pattern Anal. Mach. Intell.*, vol. 41, no. 6, pp. 1515–1530, 2018.
- [128] Y.-T. Hu, J.-B. Huang, and A. G. Schwing, "Videomatch: Matching based video object segmentation," in *Proc. Eur. Conf. Comput. Vis.*, 2018, pp. 56–73.
- [129] X. Li and C. C. Loy, "Video object segmentation with joint re-identification and attention-aware mask propagation," in *Proc. Eur. Conf. Comput. Vis.*, 2018.
- [130] H. Ci, C. Wang, and Y. Wang, "Video object segmentation by learning location-sensitive embeddings," in *Proc. Eur. Conf. Comput. Vis.*, 2018, pp. 524–539.
- [131] C. Vondrick, A. Shrivastava, A. Fathi, S. Guadarrama, and K. Murphy, "Tracking emerges by coloring videos," in *Proc. Eur. Conf. Comput. Vis.*, 2018, pp. 391–408.
- [132] W. Kay, J. Carreira, K. Simonyan, B. Zhang, C. Hillier, S. Vijayanarasimhan, F. Viola, T. Green, T. Back, P. Natsev *et al.*, "The kinetics human action video dataset," *arXiv preprint arXiv:1705.06950*, 2017.
- [133] H. Xiao, B. Kang, Y. Liu, M. Zhang, and J. Feng, "Online meta adaptation for fast video object segmentation," *IEEE Trans. Pattern Anal. Mach. Intell.*, vol. 42, no. 5, pp. 1205–1217, 2019.
- [134] P. Voigtlaender, Y. Chai, F. Schroff, H. Adam, B. Leibe, and L.-C. Chen, "Feelvos: Fast end-to-end embedding learning for video object segmentation," in *Proc. IEEE Conf. Comput. Vis. Pattern Recognit.*, 2019, pp. 9481–9490.
- [135] S. Xu, D. Liu, L. Bao, W. Liu, and P. Zhou, "Mhp-vos: Multiple hypotheses propagation for video object segmentation," in *Proc. IEEE Conf. Comput. Vis. Pattern Recognit.*, 2019, pp. 314–323.
- [136] H. Lin, X. Qi, and J. Jia, "Agss-vos: Attention guided single-shot video object segmentation," in *Proc. IEEE Conf. Comput. Vis. Pattern Recognit.*, 2019, pp. 3949–3957.
- [137] J. Johnander, M. Danelljan, E. Brissman, F. S. Khan, and M. Felsberg, "A generative appearance model for end-to-end video object segmentation," in *Proc. IEEE Conf. Comput. Vis. Pattern Recognit.*, 2019, pp. 8953–8962.
- [138] Q. Wang, L. Zhang, L. Bertinetto, W. Hu, and P. H. Torr, "Fast online object tracking and segmentation: A unifying approach," in *Proc. IEEE Conf. Comput. Vis. Pattern Recognit.*, 2019, pp. 1328–1338.
- [139] B. A. Griffin and J. J. Corso, "Bubblenets: Learning to select the guidance frame in video object segmentation by deep sorting frames," in *Proc. IEEE Conf. Comput. Vis. Pattern Recognit.*, 2019, pp. 8914–8923.
- [140] Z. Wang, J. Xu, L. Liu, F. Zhu, and L. Shao, "Ranet: Ranking attention network for fast video object segmentation," in *Proc. IEEE Int. Conf. Comput. Vis.*, 2019, pp. 3978–3987.
- [141] G. Li and Y. Yu, "Visual saliency based on multiscale deep features," in *Proc. IEEE Conf. Comput. Vis. Pattern Recognit.*, 2015, pp. 5455–5463.
- [142] X. Zeng, R. Liao, L. Gu, Y. Xiong, S. Fidler, and R. Urtasun, "Dmm-net: Differentiable mask-matching network for video object segmentation," in *Proc. IEEE Int. Conf. Comput. Vis.*, 2019, pp. 3929–3938.
- [143] L. Zhang, Z. Lin, J. Zhang, H. Lu, and Y. He, "Fast video object segmentation via dynamic targeting network," in *Proc. IEEE Int. Conf. Comput. Vis.*, 2019, pp. 5582–5591.
- [144] S. W. Oh, J.-Y. Lee, N. Xu, and S. J. Kim, "Video object segmentation using space-time memory networks," in *Proc. IEEE Int. Conf. Comput. Vis.*, 2019, pp. 9226–9235.
- [145] X. Wang, A. Jabri, and A. A. Efros, "Learning correspondence from the cycle-consistency of time," in *Proc. IEEE Conf. Comput. Vis. Pattern Recognit.*, 2019, pp. 2566–2576.
- [146] D. F. Fouhey, W.-c. Kuo, A. A. Efros, and J. Malik, "From lifestyle vlogs to everyday interactions," in *Proc. IEEE Conf. Comput. Vis. Pattern Recognit.*, 2018, pp. 4991–5000.
- [147] X. Li, S. Liu, S. De Mello, X. Wang, J. Kautz, and M.-H. Yang, "Joint-task self-supervised learning for temporal correspondence," in *Proc. Advances Neural Inf. Process. Syst.*, 2019, pp. 318–328.
- [148] T. Meinhardt and L. Leal-Taixé, "Make one-shot video object segmentation efficient again," in *Proc. Advances Neural Inf. Process. Syst.*, 2020.
- [149] Y. Liang, X. Li, N. Jafari, and Q. Chen, "Video object segmentation with adaptive feature bank and uncertain-region refinement," in *Proc. Advances Neural Inf. Process. Syst.*, 2020.
- [150] X. Huang, J. Xu, Y.-W. Tai, and C.-K. Tang, "Fast video object segmentation with temporal aggregation network and dynamic template matching," in *Proc. IEEE Conf. Comput. Vis. Pattern Recognit.*, 2020, pp. 8879–8889.
- [151] M. Sun, J. Xiao, E. G. Lim, B. Zhang, and Y. Zhao, "Fast template matching and update for video object tracking and segmentation," in *Proc. IEEE Conf. Comput. Vis. Pattern Recognit.*, 2020, pp. 10791–10799.
- [152] X. Chen, Z. Li, Y. Yuan, G. Yu, J. Shen, and D. Qi, "State-aware tracker for real-time video object segmentation," in *Proc. IEEE Conf. Comput. Vis. Pattern Recognit.*, 2020, pp. 9384–9393.
- [153] A. Robinson, F. J. Lawin, M. Danelljan, F. S. Khan, and M. Felsberg, "Learning fast and robust target models for video object segmentation," in *Proc. IEEE Conf. Comput. Vis. Pattern Recognit.*, 2020, pp. 7406–7415.
- [154] Y. Zhang, Z. Wu, H. Peng, and S. Lin, "A transductive approach for video object segmentation," in *Proc. IEEE Conf. Comput. Vis. Pattern Recognit.*, 2020, pp. 6949–6958.
- [155] Z. Lai, E. Lu, and W. Xie, "Mast: A memory-augmented self-supervised tracker," in *Proc. IEEE Conf. Comput. Vis. Pattern Recognit.*, 2020, pp. 6479–6488.
- [156] Y. Li, Z. Shen, and Y. Shan, "Fast video object segmentation using the global context module," in *Proc. Eur. Conf. Comput. Vis.*, 2020, pp. 735–750.
- [157] H. Seong, J. Hyun, and E. Kim, "Kernelized memory network for video object segmentation," in *Proc. Eur. Conf. Comput. Vis.*, 2020, pp. 629–645.
- [158] Z. Yang, Y. Wei, and Y. Yang, "Collaborative video object segmentation by foreground-background integration," in *Proc. Eur. Conf. Comput. Vis.*, 2020, pp. 332–348.
- [159] G. Bhat, F. J. Lawin, M. Danelljan, A. Robinson, M. Felsberg, L. Van Gool, and R. Timofte, "Learning what to learn for video object segmentation," in *Proc. Eur. Conf. Comput. Vis.*, 2020, pp. 777–794.
- [160] R. Wu, H. Lin, X. Qi, and J. Jia, "Memory selection network for video propagation," in *Proc. Eur. Conf. Comput. Vis.*, 2020, pp. 175–190.
- [161] Y. Li, N. Xu, J. Peng, J. See, and W. Lin, "Delving into the cyclic mechanism in semi-supervised video object segmentation," in *Proc. Advances Neural Inf. Process. Syst.*, 2020.
- [162] F. Lin, H. Xie, Y. Li, and Y. Zhang, "Query-memory re-aggregation for weakly-supervised video object segmentation," in *AAAI Conference on Artificial Intelligence*, 2021.
- [163] H. Wang, X. Jiang, H. Ren, Y. Hu, and S. Bai, "Swiftnet: Real-time video object segmentation," in *Proc. IEEE Conf. Comput. Vis. Pattern Recognit.*, 2021, pp. 1296–1305.
- [164] H. Park, J. Yoo, S. Jeong, G. Venkatesh, and N. Kwak, "Learning dynamic network using a reuse gate function in semi-supervised

- video object segmentation," in *Proc. IEEE Conf. Comput. Vis. Pattern Recognit.*, 2021, pp. 8405–8414.
- [165] B. Duke, A. Ahmed, C. Wolf, P. Aarabi, and G. W. Taylor, "Sstvos: Sparse spatiotemporal transformers for video object segmentation," in *Proc. IEEE Conf. Comput. Vis. Pattern Recognit.*, 2021.
- [166] W. Ge, X. Lu, and J. Shen, "Video object segmentation using global and instance embedding learning," in *Proc. IEEE Conf. Comput. Vis. Pattern Recognit.*, 2021, pp. 16836–16845.
- [167] L. Hu, P. Zhang, B. Zhang, P. Pan, Y. Xu, and R. Jin, "Learning position and target consistency for memory-based video object segmentation," in *Proc. IEEE Conf. Comput. Vis. Pattern Recognit.*, 2021, pp. 4144–4154.
- [168] H. Xie, H. Yao, S. Zhou, S. Zhang, and W. Sun, "Efficient regional memory network for video object segmentation," in *Proc. IEEE Conf. Comput. Vis. Pattern Recognit.*, 2021, pp. 1286–1295.
- [169] A. Jabri, A. Owens, and A. Efros, "Space-time correspondence as a contrastive random walk," in *Proc. Advances Neural Inf. Process. Syst.*, vol. 33, 2020.
- [170] X. Lu, W. Wang, J. Shen, D. Crandall, and J. Luo, "Zero-shot video object segmentation with co-attention siamese networks," *IEEE Trans. Pattern Anal. Mach. Intell.*, 2020.
- [171] X. Lu, W. Wang, J. Shen, D. Crandall, and L. Van Gool, "Segmenting objects from relational visual data," *IEEE Trans. Pattern Anal. Mach. Intell.*, 2021.
- [172] S. Caelles, J. Pont-Tuset, F. Perazzi, A. Montes, K.-K. Maninis, and L. Van Gool, "The 2019 davis challenge on vos: Unsupervised multi-object segmentation," *arXiv:1905.00737*, 2019.
- [173] J. Luiten, I. E. Zulfikar, and B. Leibe, "Unovost: Unsupervised offline video object segmentation and tracking," in *Proceedings of the IEEE/CVF Winter Conference on Applications of Computer Vision*, 2020, pp. 2000–2009.
- [174] W. Wang, J. Shen, X. Lu, S. C. Hoi, and H. Ling, "Paying attention to video object pattern understanding," *IEEE Trans. Pattern Anal. Mach. Intell.*, 2020.
- [175] K. He, G. Gkioxari, P. Dollár, and R. Girshick, "Mask r-cnn," in *Proc. IEEE Int. Conf. Comput. Vis.*, 2017, pp. 2961–2969.
- [176] A. Benard and M. Gygli, "Interactive video object segmentation in the wild," *arXiv preprint arXiv:1801.00269*, 2017.
- [177] Y. Chen, J. Pont-Tuset, A. Montes, and L. Van Gool, "Blazingly fast video object segmentation with pixel-wise metric learning," in *Proc. IEEE Conf. Comput. Vis. Pattern Recognit.*, 2018, pp. 1189–1198.
- [178] S. W. Oh, J.-Y. Lee, N. Xu, and S. J. Kim, "Fast user-guided video object segmentation by interaction-and-propagation networks," in *Proc. IEEE Conf. Comput. Vis. Pattern Recognit.*, 2019, pp. 5247–5256.
- [179] J. Miao, Y. Wei, and Y. Yang, "Memory aggregation networks for efficient interactive video object segmentation," in *Proc. IEEE Conf. Comput. Vis. Pattern Recognit.*, 2020, pp. 10366–10375.
- [180] Y. Heo, Y. J. Koh, and C.-S. Kim, "Interactive video object segmentation using global and local transfer modules," in *Proc. Eur. Conf. Comput. Vis.*, 2020.
- [181] B. Chen, H. Ling, X. Zeng, G. Jun, Z. Xu, and S. Fidler, "Scribblebox: Interactive annotation framework for video object segmentation," in *Proc. Eur. Conf. Comput. Vis.*, 2020.
- [182] Z. Yin, J. Zheng, W. Luo, S. Qian, H. Zhang, and S. Gao, "Learning to recommend frame for interactive video object segmentation in the wild," in *Proc. IEEE Conf. Comput. Vis. Pattern Recognit.*, 2021, pp. 15445–15454.
- [183] Y. Heo, Y. J. Koh, and C.-S. Kim, "Guided interactive video object segmentation using reliability-based attention maps," in *Proc. IEEE Conf. Comput. Vis. Pattern Recognit.*, 2021, pp. 7322–7330.
- [184] H. K. Cheng, Y.-W. Tai, and C.-K. Tang, "Modular interactive video object segmentation: Interaction-to-mask, propagation and difference-aware fusion," in *Proc. IEEE Conf. Comput. Vis. Pattern Recognit.*, 2021, pp. 5559–5568.
- [185] L. Wang, W. Ouyang, X. Wang, and H. Lu, "Visual tracking with fully convolutional networks," in *Proc. IEEE Int. Conf. Comput. Vis.*, 2015, pp. 3119–3127.
- [186] K. Duarte, Y. S. Rawat, and M. Shah, "Capsulevos: Semi-supervised video object segmentation using capsule routing," in *Proc. IEEE Int. Conf. Comput. Vis.*, 2019, pp. 8480–8489.
- [187] A. Vaswani, N. Shazeer, N. Parmar, J. Uszkoreit, L. Jones, A. N. Gomez, L. Kaiser, and I. Polosukhin, "Attention is all you need," in *Proc. Advances Neural Inf. Process. Syst.*, 2017.
- [188] S. Caelles, A. Montes, K.-K. Maninis, Y. Chen, L. Van Gool, F. Perazzi, and J. Pont-Tuset, "The 2018 davis challenge on video object segmentation," *arXiv preprint arXiv:1803.00557*, 2018.
- [189] N. Xu, B. Price, S. Cohen, J. Yang, and T. S. Huang, "Deep interactive object selection," in *Proc. IEEE Conf. Comput. Vis. Pattern Recognit.*, 2016, pp. 373–381.
- [190] K. Gavriluyk, A. Ghodrati, Z. Li, and C. G. Snoek, "Actor and action video segmentation from a sentence," in *Proc. IEEE Conf. Comput. Vis. Pattern Recognit.*, 2018, pp. 5958–5966.
- [191] A. Khoreva, A. Rohrbach, and B. Schiele, "Video object segmentation with language referring expressions," in *Asian Conference on Computer Vision*, 2018, pp. 123–141.
- [192] H. Wang, C. Deng, J. Yan, and D. Tao, "Asymmetric cross-guided attention network for actor and action video segmentation from natural language query," in *Proc. IEEE Int. Conf. Comput. Vis.*, 2019, pp. 3939–3948.
- [193] H. Wang, C. Deng, F. Ma, and Y. Yang, "Context modulated dynamic networks for actor and action video segmentation with language queries," in *AAAI Conference on Artificial Intelligence*, 2020, pp. 12152–12159.
- [194] K. Ning, L. Xie, F. Wu, and Q. Tian, "Polar relative positional encoding for video-language segmentation," in *IJCAI*, 2020.
- [195] B. McIntosh, K. Duarte, Y. S. Rawat, and M. Shah, "Visual-textual capsule routing for text-based video segmentation," in *Proc. IEEE Conf. Comput. Vis. Pattern Recognit.*, 2020, pp. 9942–9951.
- [196] S. Seo, J.-Y. Lee, and B. Han, "Urvos: Unified referring video object segmentation network with a large-scale benchmark," in *Proc. Eur. Conf. Comput. Vis.*, 2020.
- [197] T. Hui, S. Huang, S. Liu, Z. Ding, G. Li, W. Wang, J. Han, and F. Wang, "Collaborative spatial-temporal modeling for language-queried video actor segmentation," in *Proc. IEEE Conf. Comput. Vis. Pattern Recognit.*, 2021.
- [198] L. Ye, M. Rochan, Z. Liu, X. Zhang, and Y. Wang, "Referring segmentation in images and videos with cross-modal self-attention network," *IEEE Trans. Pattern Anal. Mach. Intell.*, 2021.
- [199] E. Shelhamer, K. Rakelly, J. Hoffman, and T. Darrell, "Clockwork convnets for video semantic segmentation," in *Proc. Eur. Conf. Comput. Vis.*, 2016, pp. 852–868.
- [200] M. Cordts, M. Omran, S. Ramos, T. Rehfeld, M. Enzweiler, R. Benenson, U. Franke, S. Roth, and B. Schiele, "The cityscapes dataset for semantic urban scene understanding," in *Proc. IEEE Conf. Comput. Vis. Pattern Recognit.*, 2016, pp. 3213–3223.
- [201] A. Kundu, V. Vineet, and V. Koltun, "Feature space optimization for semantic video segmentation," in *Proc. IEEE Conf. Comput. Vis. Pattern Recognit.*, 2016, pp. 3168–3175.
- [202] G. J. Brostow, J. Fauqueur, and R. Cipolla, "Semantic object classes in video: A high-definition ground truth database," *Pattern Recognition Letters*, vol. 30, no. 2, pp. 88–97, 2009.
- [203] J. Hur and S. Roth, "Joint optical flow and temporally consistent semantic segmentation," in *European Conference on Computer Vision*, 2016, pp. 163–177.
- [204] P. Voigtlaender, M. Krause, A. Osep, J. Luiten, B. B. G. Sekar, A. Geiger, and B. Leibe, "Mots: Multi-object tracking and segmentation," in *Proc. IEEE Conf. Comput. Vis. Pattern Recognit.*, 2019, pp. 7942–7951.
- [205] B. Mahasseni, S. Todorovic, and A. Fern, "Budget-aware deep semantic video segmentation," in *Proc. IEEE Conf. Comput. Vis. Pattern Recognit.*, 2017, pp. 1029–1038.
- [206] X. Jin, X. Li, H. Xiao, X. Shen, Z. Lin, J. Yang, Y. Chen, J. Dong, L. Liu, Z. Jie *et al.*, "Video scene parsing with predictive feature learning," in *Proc. IEEE Int. Conf. Comput. Vis.*, 2017, pp. 5580–5588.
- [207] R. Gadde, V. Jampani, and P. V. Gehler, "Semantic video cnns through representation warping," in *Proc. IEEE Int. Conf. Comput. Vis.*, 2017, pp. 4453–4462.
- [208] X. Zhu, Y. Xiong, J. Dai, L. Yuan, and Y. Wei, "Deep feature flow for video recognition," in *Proc. IEEE Conf. Comput. Vis. Pattern Recognit.*, 2017, pp. 2349–2358.
- [209] F. S. Saleh, M. S. Aliakbarian, M. Salzmann, L. Petersson, and J. M. Alvarez, "Bringing background into the foreground: Making all classes equal in weakly-supervised video semantic segmentation," in *Proc. IEEE Int. Conf. Comput. Vis.*, 2017, pp. 2125–2135.
- [210] D. Nilsson and C. Sminchisescu, "Semantic video segmentation by gated recurrent flow propagation," in *Proc. IEEE Conf. Comput. Vis. Pattern Recognit.*, 2018, pp. 6819–6828.

- [211] Y. Li, J. Shi, and D. Lin, "Low-latency video semantic segmentation," in *Proc. IEEE Conf. Comput. Vis. Pattern Recognit.*, 2018, pp. 5997–6005.
- [212] Y.-S. Xu, T.-J. Fu, H.-K. Yang, and C.-Y. Lee, "Dynamic video segmentation network," in *Proc. IEEE Conf. Comput. Vis. Pattern Recognit.*, 2018, pp. 6556–6565.
- [213] P.-Y. Huang, W.-T. Hsu, C.-Y. Chiu, T.-F. Wu, and M. Sun, "Efficient uncertainty estimation for semantic segmentation in videos," in *Proc. Eur. Conf. Comput. Vis.*, 2018, pp. 520–535.
- [214] S. Chandra, C. Couprie, and I. Kokkinos, "Deep spatio-temporal random fields for efficient video segmentation," in *Proc. IEEE Conf. Comput. Vis. Pattern Recognit.*, 2018, pp. 8915–8924.
- [215] S. Jain, X. Wang, and J. E. Gonzalez, "Accel: A corrective fusion network for efficient semantic segmentation on video," in *Proc. IEEE Conf. Comput. Vis. Pattern Recognit.*, 2019, pp. 8866–8875.
- [216] Y. Zhu, K. Sapra, F. A. Reda, K. J. Shih, S. Newsam, A. Tao, and B. Catanzaro, "Improving semantic segmentation via video propagation and label relaxation," in *Proc. IEEE Conf. Comput. Vis. Pattern Recognit.*, 2019, pp. 8856–8865.
- [217] M. Ding, Z. Wang, B. Zhou, J. Shi, Z. Lu, and P. Luo, "Every frame counts: joint learning of video segmentation and optical flow," in *AAAI Conference on Artificial Intelligence*, 2020, pp. 10713–10720.
- [218] P. Hu, F. Caba, O. Wang, Z. Lin, S. Sclaroff, and F. Perazzi, "Temporally distributed networks for fast video semantic segmentation," in *Proc. IEEE Conf. Comput. Vis. Pattern Recognit.*, 2020, pp. 8818–8827.
- [219] N. Silberman, D. Hoiem, P. Kohli, and R. Fergus, "Indoor segmentation and support inference from rgbd images," in *Proc. Eur. Conf. Comput. Vis.*, 2012, pp. 746–760.
- [220] G. Bertasius and L. Torresani, "Classifying, segmenting, and tracking object instances in video with mask propagation," in *Proc. IEEE Conf. Comput. Vis. Pattern Recognit.*, 2020, pp. 9739–9748.
- [221] D. Kim, S. Woo, J.-Y. Lee, and I. S. Kweon, "Video panoptic segmentation," in *Proc. IEEE Conf. Comput. Vis. Pattern Recognit.*, 2020, pp. 9859–9868.
- [222] L. Porzi, M. Hofinger, I. Ruiz, J. Serrat, S. R. Bulo, and P. Kotschieder, "Learning multi-object tracking and segmentation from automatic annotations," in *Proc. IEEE Conf. Comput. Vis. Pattern Recognit.*, 2020, pp. 6846–6855.
- [223] F. Yu, H. Chen, X. Wang, W. Xian, Y. Chen, F. Liu, V. Madhavan, and T. Darrell, "Bdd100k: A diverse driving dataset for heterogeneous multitask learning," in *Proc. IEEE Conf. Comput. Vis. Pattern Recognit.*, 2020, pp. 2636–2645.
- [224] C.-C. Lin, Y. Hung, R. Feris, and L. He, "Video instance segmentation tracking with a modified vae architecture," in *Proc. IEEE Conf. Comput. Vis. Pattern Recognit.*, 2020, pp. 13 147–13 157.
- [225] Y. Liu, C. Shen, C. Yu, and J. Wang, "Efficient semantic video segmentation with per-frame inference," in *Proc. Eur. Conf. Comput. Vis.*, 2020, pp. 352–368.
- [226] J. Cao, R. M. Anwer, H. Cholakkal, F. S. Khan, Y. Pang, and L. Shao, "Sipmask: Spatial information preservation for fast image and video instance segmentation," in *Proc. Eur. Conf. Comput. Vis.*, 2020.
- [227] A. Athar, S. Mahadevan, A. Ošep, L. Leal-Taixé, and B. Leibe, "Stem-seg: Spatio-temporal embeddings for instance segmentation in videos," in *Proc. Eur. Conf. Comput. Vis.*, 2020, pp. 158–177.
- [228] L.-C. Chen, R. G. Lopes, B. Cheng, M. D. Collins, E. D. Cubuk, B. Zoph, H. Adam, and J. Shlens, "Naive-student: Leveraging semi-supervised learning in video sequences for urban scene segmentation," in *Proc. Eur. Conf. Comput. Vis.*, 2020, pp. 695–714.
- [229] Y. Fu, L. Yang, D. Liu, T. S. Huang, and H. Shi, "Compfeat: Comprehensive feature aggregation for video instance segmentation," in *AAAI Conference on Artificial Intelligence*, 2021.
- [230] J. Wu, J. Cao, L. Song, Y. Wang, M. Yang, and J. Yuan, "Track to detect and segment: An online multi-object tracker," in *Proc. IEEE Conf. Comput. Vis. Pattern Recognit.*, 2021.
- [231] D. Liu, Y. Cui, W. Tan, and Y. Chen, "Sg-net: Spatial granularity network for one-stage video instance segmentation," in *Proc. IEEE Conf. Comput. Vis. Pattern Recognit.*, 2021.
- [232] Y. Wang, Z. Xu, X. Wang, C. Shen, B. Cheng, H. Shen, and H. Xia, "End-to-end video instance segmentation with transformers," in *Proc. IEEE Conf. Comput. Vis. Pattern Recognit.*, 2021.
- [233] L. Hoyer, D. Dai, Y. Chen, A. Koring, S. Saha, and L. Van Gool, "Three ways to improve semantic segmentation with self-supervised depth estimation," in *Proc. IEEE Conf. Comput. Vis. Pattern Recognit.*, 2021, pp. 11 130–11 140.
- [234] S. Woo, D. Kim, J.-Y. Lee, and I. S. Kweon, "Learning to associate every segment for video panoptic segmentation," in *Proc. IEEE Conf. Comput. Vis. Pattern Recognit.*, 2021, pp. 2705–2714.
- [235] S. Qiao, Y. Zhu, H. Adam, A. Yuille, and L.-C. Chen, "Vip-deeplab: Learning visual perception with depth-aware video panoptic segmentation," in *Proc. IEEE Conf. Comput. Vis. Pattern Recognit.*, 2021.
- [236] Q. Liu, V. Ramanathan, D. Mahajan, A. Yuille, and Z. Yang, "Weakly supervised instance segmentation for videos with temporal mask consistency," in *Proc. IEEE Conf. Comput. Vis. Pattern Recognit.*, 2021.
- [237] Y. Fu, S. Liu, U. Iqbal, S. De Mello, H. Shi, and J. Kautz, "Learning to track instances without video annotations," in *Proc. IEEE Conf. Comput. Vis. Pattern Recognit.*, 2021.
- [238] H. Lin, R. Wu, S. Liu, J. Lu, and J. Jia, "Video instance segmentation with a propose-reduce paradigm," in *Proc. IEEE Int. Conf. Comput. Vis.*, 2021, pp. 1739–1748.
- [239] J. Gao, C. Sun, Z. Yang, and R. Nevatia, "Tall: Temporal activity localization via language query," in *Proc. IEEE Int. Conf. Comput. Vis.*, 2017, pp. 5267–5275.
- [240] L. Anne Hendricks, O. Wang, E. Shechtman, J. Sivic, T. Darrell, and B. Russell, "Localizing moments in video with natural language," in *Proc. IEEE Int. Conf. Comput. Vis.*, 2017, pp. 5803–5812.
- [241] Z. Li, R. Tao, E. Gavves, C. G. Snoek, and A. W. Smeulders, "Tracking by natural language specification," in *Proc. IEEE Conf. Comput. Vis. Pattern Recognit.*, 2017, pp. 6495–6503.
- [242] G. E. Hinton, S. Sabour, and N. Frosst, "Matrix capsules with em routing," in *Proc. Int. Conf. Learn. Representations*, 2018.
- [243] S. Liu, T. Hui, S. Huang, Y. Wei, B. Li, and G. Li, "Cross-modal progressive comprehension for referring segmentation," *IEEE Trans. Pattern Anal. Mach. Intell.*, 2021.
- [244] A. Hu, A. Kendall, and R. Cipolla, "Learning a spatio-temporal embedding for video instance segmentation," in *Proc. Int. Conf. Learn. Representations*, 2019.
- [245] Y. Xiong, R. Liao, H. Zhao, R. Hu, M. Bai, E. Yumer, and R. Urtasun, "Upsnet: A unified panoptic segmentation network," in *Proc. IEEE Conf. Comput. Vis. Pattern Recognit.*, 2019, pp. 8818–8826.
- [246] J. Miao, Y. Wei, Y. Wu, C. Liang, G. Li, and Y. Yang, "Vspw: A large-scale dataset for video scene parsing in the wild," in *Proc. IEEE Conf. Comput. Vis. Pattern Recognit.*, 2021.
- [247] J. Qi, Y. Gao, Y. Hu, X. Wang, X. Liu, X. Bai, S. Belongie, A. Yuille, P. Torr, and S. Bai, "Occluded video instance segmentation," *arXiv preprint arXiv:2102.01558*, 2021.
- [248] S. D. Jain and K. Grauman, "Supervoxel-consistent foreground propagation in video," in *Proc. Eur. Conf. Comput. Vis.*, 2014, pp. 656–671.
- [249] C. Xu, S.-H. Hsieh, C. Xiong, and J. J. Corso, "Can humans fly? action understanding with multiple classes of actors," in *Proc. IEEE Conf. Comput. Vis. Pattern Recognit.*, 2015, pp. 2264–2273.
- [250] H. Jhuang, J. Gall, S. Zuffi, C. Schmid, and M. J. Black, "Towards understanding action recognition," in *Proc. IEEE Int. Conf. Comput. Vis.*, 2013, pp. 3192–3199.
- [251] A. Geiger, P. Lenz, and R. Urtasun, "Are we ready for autonomous driving? the kitti vision benchmark suite," in *Proc. IEEE Conf. Comput. Vis. Pattern Recognit.*, 2012, pp. 3354–3361.
- [252] A. Milan, L. Leal-Taixé, I. Reid, S. Roth, and K. Schindler, "Mot16: A benchmark for multi-object tracking," *arXiv preprint arXiv:1603.00831*, 2016.
- [253] S. R. Richter, Z. Hayder, and V. Koltun, "Playing for benchmarks," in *Proc. IEEE Int. Conf. Comput. Vis.*, 2017, pp. 2232–2241.
- [254] N. Märki, F. Perazzi, O. Wang, and A. Sorkine-Hornung, "Bilateral space video segmentation," in *Proc. IEEE Conf. Comput. Vis. Pattern Recognit.*, 2016, pp. 743–751.
- [255] D. R. Martin, C. C. Fowlkes, and J. Malik, "Learning to detect natural image boundaries using local brightness, color, and texture cues," *IEEE Trans. Pattern Anal. Mach. Intell.*, vol. 26, no. 5, pp. 530–549, 2004.
- [256] S. Belongie, J. Malik, and J. Puzicha, "Shape matching and object recognition using shape contexts," *IEEE Trans. Pattern Anal. Mach. Intell.*, no. 4, pp. 509–522, 2002.
- [257] W. Wang, M. Feiszli, H. Wang, and D. Tran, "Unidentified video objects: A benchmark for dense, open-world segmentation," in *Proc. IEEE Int. Conf. Comput. Vis.*, 2021, pp. 10776–10785.
- [258] E. Bengio, P.-L. Bacon, J. Pineau, and D. Precup, "Conditional computation in neural networks for faster models," in *Proc. Int. Conf. Learn. Representations*, 2016.